DEVELOPMENT OF CALCIUM-POLYPHOSPHATE PARTICLES FOR THERAPEUTIC DELIVERY IN THE JOINT

Janani Mahendran

A thesis submitted to the Faculty of Graduate and Postdoctoral Studies

in partial fulfillment of the requirements for the degree of

MASTER OF APPLIED SCIENCE

in Chemical and Biological Engineering

Faculty of Engineering

University of Ottawa

Ottawa, Canada

December 2019

Abstract

Osteoarthritis (OA) is the most common type of joint disease that affects nearly 5 million people in Canada alone. OA involves degenerative processes affecting the integrity of articular cartilage, a thin soft tissue at the surface of subchondral bones in joints that facilitates smooth and frictionless movement. This disease also affects the other tissues of the joint, including the synovium and its resident cells the fibroblast-like and macrophage-like synoviocytes. Consequences of this pathology include painful movement and stiff joints resulting in loss of range of motion. A broad number of factors may contribute to the development of OA, including obesity, injuries, infections, genetic predispositions and aging. Although there are a number of medications used for the treatment of OA, these only serve to manage its symptoms. An actual cure is yet to be developed. Inorganic polyphosphate (polyP) has previously been identified as a potentially interesting biomolecule for the treatment of OA because of its ability to stimulate tissue formation by chondrocytes - the cells found in the articular cartilage. In this thesis, we first aimed to evaluate the potential of polyP as a therapeutic for joint diseases such as OA further, by characterizing its effects on a number of cell processes (e.g., proliferation, metabolic activity, migration, matrix accumulation) in fibroblast-like synoviocytes (FLS) - specialized cells found in the synovium encapsulating the synovial joints. The synovium is an important tissue for joint physiology and OA pathogenesis; it is thus essential that any therapeutic introduced in the joint not impact this tissue negatively. These studies showed that polyP significantly inhibits FLS proliferation. This effect is interesting in the context of OA as FLS proliferation is associated with progression of the disease. PolyP also increased FLS migration rate and caused changes in metabolic activity, although the trends were inconsistent over time. We also optimized a new protocol for the synthesis of sub-micron calcium-polyP particles. Nanoparticle drug delivery for

OA treatment has been gaining importance in recent years as a way to access the cells in cartilage through the small pores in the extracellular matrix (ECM) and increase drug retention time in the joint. The calcium-polyP particles were synthesized by drop-wise addition of polyP into a calcium solution at controlled pH, drop rate and mixing rate. Particles size and stability before and after sterilization were measured by dynamic light scattering. We showed that the addition of sodium citrate dihydrate as a capping agent largely prevented particle agglomeration and increased particle stability. Control over particle size, particularly in the nanometer scale, remains to be achieved; however, this work is a first step towards the development of polyP delivery systems for the treatment of OA.

Résumé

L'arthrose est le type de maladie articulaire le plus courant qui touche près de 5 millions de personnes au Canada seulement. Cette condition implique des processus dégénératifs qui affectent l'intégrité du cartilage articulaire, une mince couche de tissu flexible qui se trouve à la surface des os sous-chondraux dans les articulations et qui facilite un mouvement fluide et à faible friction. Cette maladie affecte aussi les autres tissus de l'articulation, y compris la membrane synoviale et ces cellules résidents, les synoviocytes de types fibroblastes et les synoviocytes de types macrophages. Les conséquences de cette pathologie incluent des mouvements douloureux et des articulations raides, entraînant une perte de l'amplitude des mouvements. Un grand nombre de facteurs contribuent au développement de l'arthrose, notamment l'obésité, les blessures, les infections, les prédispositions génétiques et le vieillissement. Malgré qu'un certain nombre de médicaments soient utilisés pour son traitement, ceux-ci ne servent qu'à réduire les symptômes. Un véritable remède permettant d'interrompre la progression de la pathologie doit encore être développé. Le polyphosphate inorganique (polyP) a déjà été identifié comme une biomolécule potentiellement intéressante pour le traitement de l'arthrose en raison de sa capacité à stimuler la formation de tissus cartilagineux par les chondrocytes - les cellules présentes dans le cartilage. Dans cette thèse, nous avons d'abord visé l'évaluation du potentiel du polyP en tant que molécule thérapeutique pour les maladies des articulations tel que l'arthrose, en caractérisant ses effets sur un certain nombre de processus cellulaires (i.e. prolifération, activité métabolique, migration, accumulation de la matrice), sur les synoviocytes de type fibroblaste (FLS) - cellules spécialisées trouvées dans la membrane synoviale encapsulant les articulations synoviales. Le synovium est un tissu important pour la physiologie des articulations et la pathogenèse de l'arthrose ; il est donc essentiel que tout

traitement thérapeutique introduit dans l'articulation ne produise pas d'impact négatif sur ce tissu. Ces études ont montré que le polyP inhibe considérablement la prolifération des FLS. Cet effet est intéressant dans le contexte de l'arthrose vu que la prolifération des FLS est associée avec la progression de cette maladie. PolyP a aussi augmenté le taux de migration des FLS, et a causé des changements dans l'activité métabolique, bien que les modèles ne soient pas uniformes. Nous avons également optimisé un nouveau protocole pour synthétiser des particules de calcium-polyP de taille submicrométriques. L'administration des médicaments à l'aide de nanomatériaux pour le traitement de l'arthrose a pris de l'importance ces dernières années en tant que moyen d'accéder aux cellules du cartilage par les petits pores de la matrice extracellulaire et d'ainsi augmenter le temps de rétention des médicaments dans l'articulation. Les particules de calcium-polyP ont été synthétisées par addition du polyP dans une solution de calcium à pH, débit et taux de mélange contrôlés. La taille et la stabilité des particules avant et après stérilisation ont été mesurées par diffusion dynamique de la lumière. Nous avons montré que l'addition du citrate de sodium déshydraté comme agent de capsulement a empêché l'agglomération des particules et a augmenté la stabilité des particules. Le contrôle de la taille des particules, en particulier dans l'échelle nanométrique, reste à réaliser. En revanche, ce travail est une première étape vers le développement d'un système de distribution polyP pour le traitement de l'arthrose.

Statement of Originality

All the contents presented in this thesis document are the product of the original work done by the author under the supervision of Dr. Jean-Philippe St-Pierre at the University of Ottawa in the Department of Chemical and Biological Engineering in partial fulfillment of the requirements for the degree of Master of Applied Science (Chemical Engineering) at the University of Ottawa. This work has been presented in/as:

1. 3-minute Thesis competition held on March 13, 2018 at the University of Ottawa.
2. Poster entitled "Development of Calcium polyphosphate particles for therapeutic delivery in the joint" by Ms. Janani Mahendran, Mr. Justin Quan and Dr. Jean-Philippe St-Pierre at the Graduate Engineering poster competition held on March 06, 2019 at the University of Ottawa.
3. Poster with the same title presented at the 35th Annual Meeting of the Canadian Biomaterials Society in Quebec City on May 22, 2019.

Statement of Contribution

This thesis document was entirely written by the author and reviewed by her supervisor, Dr. Jean-Philippe St-Pierre. The work presented in the thesis was largely performed by the author. The studies on the investigation of polyphosphate action on fibroblast-like synoviocytes cells are entirely her work. Early work toward the development of the sub-micron calcium-polyphosphate particles involved Mr. Justin Quan as part of his 4th year undergraduate thesis project; however, the data presented on this topic in this thesis was performed by the author.

I would like to dedicate this thesis to the memory of my Grandma who is no more but was always there by my side during the difficult and happy moments of my life.

Acknowledgement

I would first like to thank Dr. Jean-Philippe St-Pierre for continuously supporting and guiding me throughout my thesis journey and I was indeed grateful for being supervised by him. I would like to thank my parents and my sister for being a source of constant support, encouragement and above all for believing in me. I would like to take this opportunity to thank Dr. Xudong Cao and his students Taisa, Holly, Hesham, Yubo, Xingkai for their constant support, as well as Dr. Christoper Lan, Dr. Sidney Omelon and Matthew from Dr. Roberto Chica's lab for all their help. I wish to thank my lab colleagues, the people who were with me all the time and cheered me up whenever I felt down: Denis Viera Rey, Noor Ghadie, Justin Quan, Nimrah Munir, Josh Yazbeck, Jordan Nhan, Sean Vidotto, Jacob Boisvert, Shreya Nagavalli, Neelabh Rastogi, Jean-Pascal Bourassa, Maude Tremblay and Sietske Barnes. Thanks to my best buddies Eddy and Ramki for always being beside me and enduring me. I would like to thank all professors, non-teaching staff and members especially from the Department of Chemical and Biological Engineering for helping me out in some way or the other. A big thanks to every single person who helped me come here to Canada to pursue my studies and making something beyond my imagination a reality now.

Table of Contents

List of Abbreviations

2D	2-dimentional
AC	Articular cartilage
BSA	Bovine serum albumin
CH	Chitosan
CMP	Cartilage matrix protein
CO_2	Carbon di-oxide
COMP	Cartilage oligomeric matrix protein
CrmA	Cytokine response modifier A
DAPI	Diamidino-2-phenylindole
DEAE	Diethyl ethylamine
DEX	Dexamethasone
DLS	Dynamic light scattering
DMEM	Dulbecco's Modified Eagle's Medium
DMOAD	Disease modifying Osteoarthritis drugs
DNA	Deoxyribonucleic acid
DS	Diclofenac sodium
dsDNA	Double stranded deoxyribonucleic acid
DSPC	1,2-distearoyl-*sn-glycero*-3-phosphocholine
ECM	Extracellular matrix
EDTA	Ethylenediaminetetraacetic acid
EdU	5-ethynyl-2'-deoxyuridine
EV	Extracellular vesicles
FBS	Fetal Bovine Serum
FGF	Fibroblast growth factor
FITC	Fluorescein Isothiocyanate
FLS	Fibroblast-like synoviocytes
GAG	Glycosaminoglycans
GNP	Gold nanoparticles
HA-CS np's	Hyaluronic Acid-Chitosan nanoparticles
IA	Intra articular
IL-1β	Interleukin-1β
iNOS	Inducible nitric oxide synthase
MSC's	Mesenchymal cells

MTT	3-(4,5-dimethylthiazol-2-yl)-2,5-diphenyltetrazolium bromide
MTX	Methotrexate
NADH	Nicotinamide adenine dinucleotide hydrogen
nm	Nanometer
NO	Nitric oxide
OA	Osteoarthritis
PBS	Phosphate buffered saline
PCM	Pericellular matrix
PDI	Poly dispersity index
PEG	Polyethylene glycol
PLGA	Poly(lactic-co-glycolic acid)
polyP	Polyphosphate
RA	Rheumatoid Arthritis
SC	Sodium citrate (dihydrate)
SDS	Sodium dodecyl sulphate
SEM	Scanning electron microscopy
siRNA	Small interfering Ribonucleic acid
TA	Triamcinolone acetonide
TNF-α	Tumor necrosis factor-alpha
TRITC	Tetramethyl rhodamine

List of Tables

List of Figures

CHAPTER 1 – INTRODUCTION

Articular cartilage (AC) is a highly specialized connective tissue of the synovial joint that provides a smooth lubricating surface between opposing bones elements, while absorbing and distributing forces transferred during movement [1, 2]. This 2-4 mm thick tissue on the articulating surfaces of bone is uniquely devoid of blood vessels and nerves, which contributes to a limited intrinsic capacity for healing and repair along with the poor migration capacity of its cells, the chondrocytes [1]. As such, AC is susceptible to acute injuries and chronic diseases such as Osteoarthritis (OA). OA is the most common type of joint disease, affecting the quality of life of almost 5 million individuals in Canada, notably by leading to the progressive degeneration of the AC layer, thus causing pain and loss of mobility [3]. This degeneration is the result of unbalanced extracellular matrix (ECM) synthesis and degradation processes [4]. OA is a multivariate disease, such that its pathogenesis can be caused by a range of factors ranging from abnormal joint loading, to environmental and genetic factor, as well as aging [3]. Importantly, OA is not only a disease of the AC, but also involves changes in the other tissues of the joint including the subchondral bone and the synovium. The synovium is a specialized connective tissue lining the diarthrodial joint capsule. This tissue is responsible for producing the synovial fluid, which contributes to the lubrication of the joint and participates in joint homeostasis and inflammation. Through its production of the synovial fluid from plasma, it also plays a critical role in chondrocyte nutrition, as AC is not supplied by a vascular network.

There is currently no cure for OA; however, a number of disease-modifying OA drug (DMOAD) candidates are currently being evaluated in clinical studies [2]. Key reasons to explain the absence of a cure for OA include the complexity of the disease itself, an unresolved pathophysiology, and the fact that orally and intravenously administered drugs do not easily

reach articular cartilage owing to its avascular nature, while intra-articular injection leads to rapid clearance of the therapeutics from the joint within a matter of hours [18]. As such, ensuring that a drug is retained in the joint at therapeutic concentrations for prolonged periods of time is necessary and drug delivery systems are increasingly receiving attention for OA treatment. In the meantime, a number of therapeutics are available to clinicians to help manage the symptoms of the disease. Cell and tissue-based surgical interventions are also an active area of research for the repair of damaged or diseased AC, but the short-term relief of current technologies does not avert the need for joint replacement surgeries with permanent metallic implants [5].

Our group is studying the therapeutic potential of inorganic polyphosphate (polyP) for the treatment of OA. This polymer of orthophosphate residues is a poorly studied biomolecule that is present in organisms across the different branches of the phylogenetic tree, including in many mammalian tissues [6]. It has been shown to elicit a broad range of biological activities from acting as chelating agents, to acting as a source of energy and stabilizing growth factors [6]. It was previously shown by Dr. St-Pierre and his colleagues that polyP stimulates ECM accumulation in chondrocytes and cartilage explant cultures [6]. In another study, they showed that biweekly intra-articular injection of this biomolecule can reduce the signs of OA in a guinea pig model of the disease.

1.1. Thesis Hypotheses

While polyP exhibits a number of biological effects on chondrocytes, the resident cells of AC, its effects on cells of many of the other tissues of synovial joints remain entirely unexplored. Here, we hypothesized that, given the ubiquity of polyp in mammalian tissues and its many observed biological functions, it will impact cellular processes in fibroblast-like synoviocytes (FLS), one of the two main cell types in the synovium. Characterizing the effects of polyP on FLS is important given the role played by this lining of the joint capsule in the physiological and pathological processes of the joint. We also hypothesized that

polyP could be complexed with calcium to form stable sub-micron particles that could serve as a platform biomaterial for polyP delivery in the body.

1.2. Thesis Objectives

In order to test these hypotheses, the work in this thesis tackles two main objectives:

1. Characterize the responses of FLS to incubation with different concentrations of polyP, including proliferation, metabolic activity, migration, and extracellular matrix (ECM) accumulation.
2. Develop a protocol to synthesize stable calcium-polyP particles and characterize their size.

1.3. Thesis Organization

This thesis is divided into 6 chapters. **Chapter 2** presents a review of the literature pertinent to the studies carried out over the course of the project from a description of articular cartilage, to joint injuries and disease, current treatments for these conditions, drug delivery systems for the joint, and polyP in biology. **Chapter 3** details all the methods employed in the studies. **Chapters 4 and 5** present the results obtained for Objectives 1 and 2, respectively. Finally, **Chapter 6** provides the main conclusions resulting from the analysis of the thesis results and proposes future directions for the project.

CHAPTER 2 – LITERATURE REVIEW

2.1. Articular Cartilage (AC)

2.1.1. Functions of AC

AC is a thin layer (2-4 mm thickness in humans [1] [6]) of hyaline cartilage covering the articulating ends of bones in synovial joints (Figure 2.1). It is composed of a complex, anisotropic and highly hydrated ECM, the composition and organization of which give it its unique properties. The ECM is interspersed with specialized cells called chondrocytes that help maintain the integrity of the tissue over time by balancing intricately controlled anabolic and catabolic processes. This tissue is avascular, aneural and alymphatic in nature. The principle function of the AC is to provide a smooth lubricated, near frictionless surface for articulation and thus facilitate joint movement. It also acts to absorb forces applied through the joint during activity and distribute them more evenly across the tissue [1].

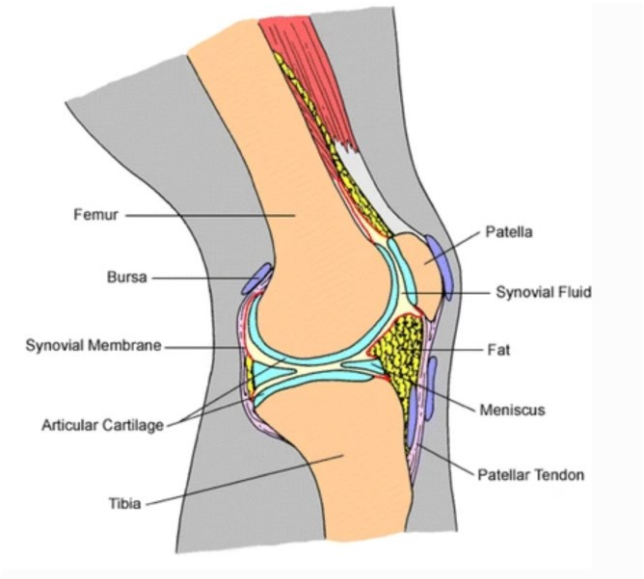

Figure 2.1. Articular cartilage location in a knee joint [25]. Licence number: 4727781107660.

2.1.2. Composition of the AC ECM

The ECM in AC is comprised of insoluble macromolecules filled with interstitial fluid, which accounts for as much as 65 to 80% of total wet weight of AC [1]. The 2 main macromolecular components of the ECM in AC are collagens and proteoglycans, and many non-collagenous proteins, as well as other biomolecules are also present as minor components [1]. The organization of these components is complex and anisotropic. These compositional and organizational aspects of AC structure will be detailed in the following subsections.

2.1.2.1. Collagens

The most abundant structural macromolecules in the ECM of AC are collagens, which can account for up to 60% of the dry weight of the tissue [1]. Collagen type II makes up to 90-95% of the collagen content, while other minor collagen types, specifically collagen types I, IV, V, VI, IX, X and XI are also present [1]. Collagen type II is the primary fibrillar component of the AC ECM, where it resists swelling and provides tensile strength to the tissue [1] [2]. Collagens type IX and XI are both involved in controlling the self-assembly of collagen type II [1] [2]. Collagen type VI is preferentially found in a compositionally distinct region of the tissue directly surrounding the chondrocytes termed pericellular matrix, where it helps transmit mechanical signals from the ECM to the cells [3] [2]. While collagen type X is located in the deeper zone of AC, its functions within the tissue still remain unresolved [3]. All members of the collagen family are composed of 3 polypeptide chains self-assembled into a triple helix, owing to the repeating glycine-X-Y amino acid sequence, where X is often proline and Y is hydroxyproline, providing stability with the help of hydrogen bonding.

2.1.2.2. Proteoglycans

The second major component of the ECM of AC is proteoglycans, which are macromolecules composed of a protein core covalently linked to polysaccharides termed glycosaminoglycans (GAG) [2]. GAG molecules are highly negatively charged, such that they attract high concentrations of cations within the ECM of the tissue. This has the effect of increasing the osmotic pressure inside the tissue, which contributes to the high-water content of the tissue in a phenomenon called the Donnan effect [7]. The expansion of hydrated proteoglycans is countered by its collagen fibril network, such that the ratio between these two components is an important factor dictating the compression properties of the tissue.

Aggrecan is the most abundant proteoglycan in AC, where it is covalently bound to chondroitin sulphate and keratin sulphate GAG polysaccharide chains [2]. It also interacts with the GAG hyaluronan via the link protein to form large proteoglycan aggregates. Its main function is to resist comprehensive loads, as a major player in the previously described Donnan effect. Other proteoglycans such as biglycan, decorin and fibromodulin are also found in lesser amount and may play roles in ECM assembly, amongst other functions [2].

2.1.2.3. Non-collagenous proteins

A host of non-collagenous molecules, which includes fibronectin, laminins, anchorin CII, cartilage matrix protein (CMP) and cartilage oligomeric matrix protein (COMP) are also present in small amounts where they play roles in matrix assembly and cell-ECM signaling.

2.1.2.4. Chondrocytes

Chondrocytes are specialized cells of cartilage tissue that differentiate from the condensation of mesenchymal cells during embryogenesis [8]. They are sparsely distributed, representing as little as 2% of the tissue volume in adults [9]. As such, chondrocytes typically do not experience cell-

cell contact and communication. They are the only cell type of AC; however, they have very different phenotypes based on their location in the AC and have thus been divided into sub-populations based on their depth: superficial, mid- and deep zone chondrocytes [9]. These cells have the ability to respond to a range of stimuli from chemical signals (e.g., growth factors, cations), to mechanical forces, and interactions with ECM molecules. The replicating potential of chondrocytes is typically very low in mature cartilage [2] [4] [9].

2.1.2.5. Extracellular vesicle (EVs)s

Owing to the avascular nature of AC and the isolation of chondrocytes discussed above, cell-to-cell communication mechanisms must involve diffusion through the dense ECM. Chondrocytes and other cells of the joint have been shown to release EVs. These structures have been suggested as transport structures for biomolecular signals between cells within a tissue and from one tissue to another. EVs have been classified in three categories: (i) exosomes that are produced by multivesicular endosomes and range in size between 30 and 150 nm, (ii) microvesicles that are formed by cell membrane budding and are typically larger with sizes ranging between 50 and 1000 nm, and (iii) apoptotic bodies [10] [11]. In cartilage, EVs have been extensively studied for their role in ECM calcification [12] [13] and to a lesser extent for inter-tissue signaling within the joint [14] [15] [16]. Further characterization of these native delivery vehicles to understand the mechanisms by which EVs are transported through cartilage, including the importance of size and surface properties, is critical in order to guide the development of biomaterials-based drug delivery systems for the treatment of cartilage and joint pathologies.

2.1.3. Organization of the AC ECM

AC is organized anisotropically with regards to both depth from the tissue surface and distance

from chondrocytes. These spatial differences in tissue composition and biomolecular assembly and organization are critical to AC functions and homeostasis. The spatial organization of AC will be described in more details.

2.1.3.1. Depth-dependent organization of AC

The depth of AC has been divided into four main zones based on ECM composition, organization and cellular phenotype, namely the superficial zone, middle zone, deep zone and the zone of calcified cartilage (Figure 2.2). In reality, the lines separating these zones are not clear and gradients in composition and organization exist [17].

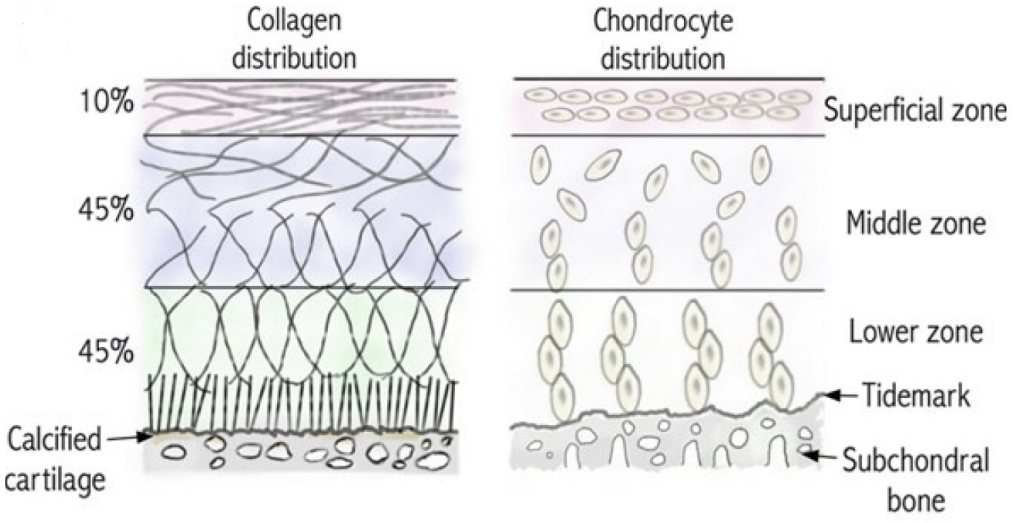

Figure 2.2. Zonal arrangement of AC with differences in collagen orientation and cell phenotype amongst many [26]. Licence number: 4727780805303.

The first layer of AC from its surface is the superficial zone, which constitutes about 10 to 20% of the total thickness. Chondrocytes in this zone are elongated in shape, more numerous and synthesize molecules involved in the lubrication of the joint including superficial zone protein also known as lubricin [2]. The density of ECM is high in this zone and the collagen fibers (primarily collagens type II and type IX) are tightly packed and aligned parallel to the articular

surface [4] [19]. This zone is in contact with the synovial fluid and is responsible for resisting the shear and tensile forces imposed by the articulation of the joints. It represents the first barrier for the diffusion of drugs and other small molecules from the synovial fluid to chondrocytes.

The second layer is the middle zone, which constitutes approximately 40 to 60% of the tissue thickness [2] [9]. This zone is composed of thick and more randomly oriented collagen fibrils and has a high proteoglycan content, which contributes to the ability of the tissue to resist compressive forces. The chondrocytes are usually spherical and more dispersed than in the superficial zone.

The deep zone constitutes 30 to 40% of the total thickness of AC and is responsible for providing the greatest amount of resistance to compressive forces applied during articulation [1] [2] [9]. It comprises collagen fibrils with the largest diameter in a radial disposition, with the highest proteoglycan content and the lowest water content [2] [9]. The chondrocytes in this zone are typically arranged in a columnar orientation parallel to the collagen fibrils and are hypertrophic. They express molecules specific to the deep zone including collagen type X and others involved in the control of tissue mineralization such as alkaline phosphatase.

The organization of each zone into a dense ECM and its composition, including the presence of a high density of polyanionic macromolecules have implications for the design of biomaterials-based strategies to deliver drugs to chondrocytes. Indeed, low sub-micron and nanometer scale particles can more easily penetrate the ECM, while a positively charged surface can also contribute positively to tissue penetration.

2.1.3.2 Organization of AC based on distance from chondrocyte

Chondrocytes are surrounded by 3 distinct layers of ECM, namely the pericellular matrix (PCM), the territorial matrix, and the interterritorial matrix [20]. These layers are characterised by their

proximity to the chondrocytes and their functions. The PCM is present in direct contact with the chondrocytes. It is abundant in type VI collagen [20]. The main function of PCM is enabling the transmission of mechanical and biomechanical signals from the ECM to the chondrocytes [20]. The layer adjacent to the PCM is the territorial matrix of the AC. A high aggrecan content in this region helps provide hydrodynamic protection against mechanical loads [20]. Further from the chondrocytes is the interterritorial matrix, which is characterized by an increased presence of degraded aggrecan molecules [20]. The interterritorial matrix helps provide the AC with its bulk mechanical properties.

2.2. OA

OA is one among the most prevalent type of joint disease. In Canada alone, it affects the quality of life of almost 5 million individuals and this number is projected to increase in coming years because of population aging and increased incidence of obesity amongst other reasons [22] [23]. OA is often presented as the progressive softening, erosion and eventual degeneration of the AC layer in the joint; however, it also leads to changes in the subchondral bone tissue, the thickening of the synovial membrane and the formation of bone spurs, as well as changes to the other tissues of the joint, such that it cannot be simply considered as a disease of AC [2, 24]. Figure 2.3 illustrates some of these changes associated with OA in the joint. The consequence of these changes for patients is pain, even at rest, and loss of range of motion in the affected joints due to stiffening.

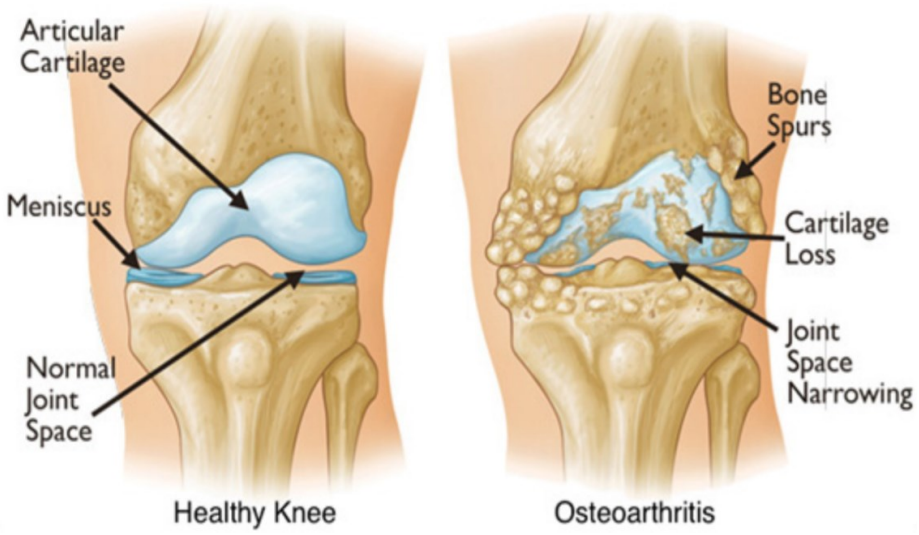

Figure 2.3. Structural differences between a normal, healthy knee and knee affected with OA [25]. Licence: Venkatesh Ponemone et al. (open access).

2.2.1. OA causes and effects

OA is a multivariate disease that can be caused by a broad range of factors. These factors are typically grouped into two main categories. First are the factors that lead to changes in the biomechanics of the joint. These may cause otherwise normal AC to sustain abnormal loading over prolonged periods and can result the progressive degeneration of the AC layer, as well as other OA-associated changes in the joint. Injuries sustained in accidents or during sports activities, as well as obesity are examples of factors that fall under this category. The second group includes factors that lead to abnormal tissues that are unable to withstand normal loading. Genetic and environmental elements, as well as lifestyle choices such as the use of cigarettes are included in this category.

While the pathological processes involved with OA are not yet fully understood, one important outcome is the loss of balance between anabolic (e.g., ECM synthesis) and catabolic (e.g., ECM degradation) processes in favor of catabolism [23]. The pathogenesis of OA

eventually leads to the rupturing of the synovial membrane due to prolonged and continuous degradation which eventually leads to inflammation. The histological pattern of synovium in OA patients is characterized by synovial lining hyperplasia, sublining fibrosis and stromal vascularization as a result of which the friction co-efficient during the movement of joints increases resulting in severe pain.

2.2.2. Clinical treatments for OA

There are currently no disease-modifying OA drugs (DMOADs) on the market. In other words, no current therapeutic drug has been shown to stop or revert the progression of OA in patients. It is important to mention that a number of pharmacological agents are currently undergoing clinical trials as DMOADs candidates. These include the inducible nitric oxide synthase (iNOS) inhibitor Cindunistat, the interleukin 1β inhibitor diacerin, oral salmon calcitonin, strontium ranelate, a truncated recombinant human fibroblast growth factor 18 sprifermin, and recombinant human bone morphogenetic protein 7 eptotermin alfa [28] [29] [30] [31] [32] [33].

2.2.2.1 Conservative OA treatments

Because of this situation, conservative treatments available to clinicians aim to help the patients manage their symptoms, including pain, swelling and joint stiffness of joints. These include physical exercises, weight loss regimens, other lifestyle changes and the use of pain and anti-inflammatory medications, such as Nonsteroidal Anti-Inflammatory Drugs (NSAIDs) [2] [24]. Aspirin, ibuprofen, and naproxen are few common examples of NSAID's available. Another conservative treatment is viscosupplementation, which involves the injection of a lubricating fluid such as a solution of hyaluronic acid within the synovial capsule of affected joints to ease movement and reduce pain [24]. This procedure needs to be repeated every few months to continue being effective. The clinical data from intra-articular injections of hyaluronic acid are

being re-analyzed with the aim of establishing it as a DMOAD [34].

2.2.2.2. Surgical interventions for treatment of damaged AC

Cell- and tissue-based strategies have been developed to stimulate the production of repair tissue at sites of damaged cartilage. These include marrow stimulation surgeries, autologous chondrocyte implantation (ACI), matrix-assisted chondrocyte implantation (MACI), and mosaicplasty.

Marrow stimulation (Figure 2.4) is currently the "gold standard" intervention for AC repair and is performed more than 100,000 times per year around the world [35]. This surgical procedure involves removing the damaged cartilage from a focal defect in a step called debridement, which is sometimes performed as a stand-alone surgery, followed by the creation of small fractures in the subchondral bone to access the bone marrow. The bleeding occurring in the defect allows the formation of a blood clot that serves as a scaffold for infiltration by bone marrow stromal cells. These cells deposit fibrocartilaginous repair tissue in the defect, the composition of which leads to inferior mechanical properties than AC [35].

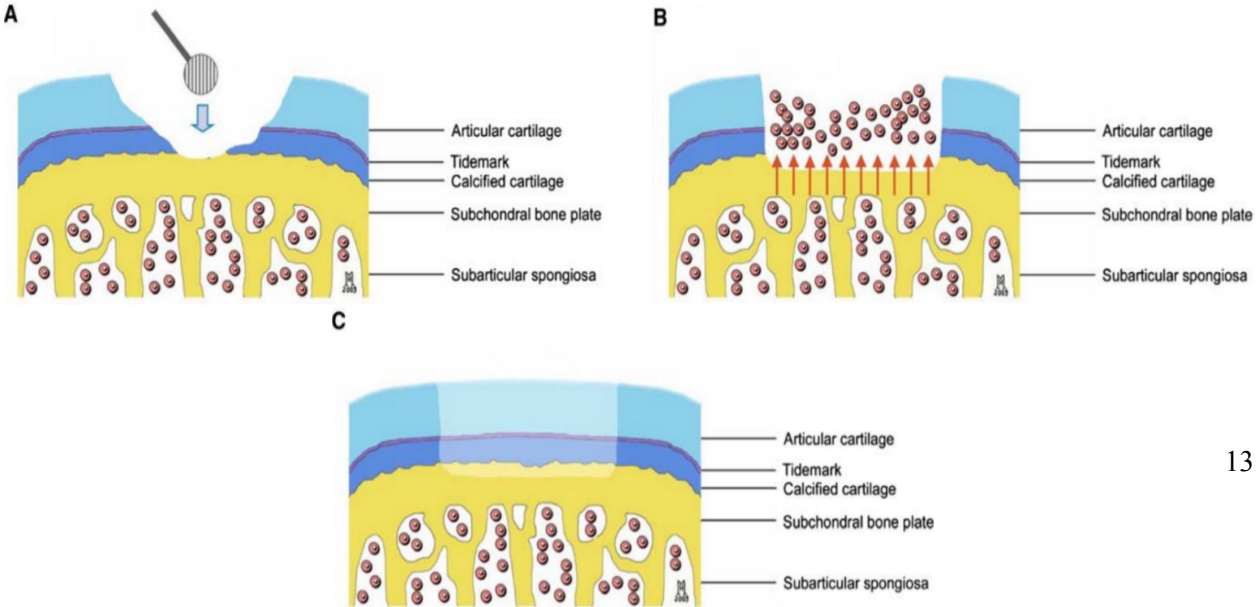

Figure 2.4. Schematic of the marrow stimulation procedure. (A) The defect is cleaned (debridements). (B) Abrasion allows to remove approximately 1 mm of subchondral bone, resulting in bleeding in the defect, as an example of marrow stimulation strategy.(C) Fibrocartilaginous repair fills the defect [35]. Licence number: 4655070698186.

ACI is a procedure that requires two separate surgeries and is currently not allowed in Canada (Figure 2.5). In the first surgery, AC is removed from a non-load bearing area of the joint and digested enzymatically to release the chondrocytes. These cells are allowed to proliferate in vitro to produce a large enough number of cells to repair the damaged AC site. A second surgery then allows the debridement of the damaged tissue and the creation of a "pouch" over the defect, often with the use of a peritoneal membrane isolated from the surface of adjacent bone, and injection of the amplified chondrocytes in the "pouch" [36]. The need for two surgeries and an in vitro cell amplification stage make this surgical intervention an expensive option. Furthermore, chondrocytes are known to dedifferentiate when cultured in vitro for amplification, such that the tissue produced may be of inferior quality to AC [1] [36].

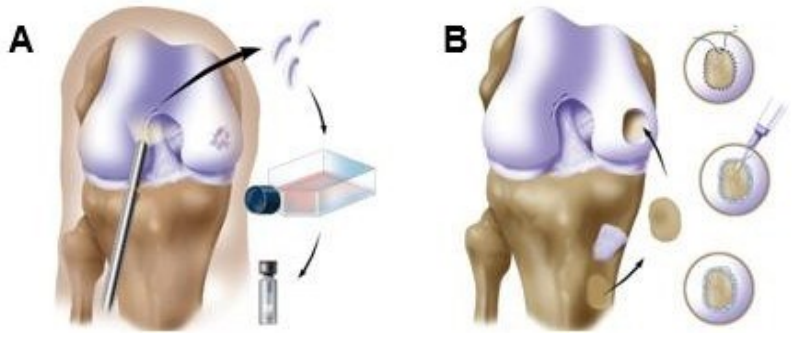

Figure 2.5. Illustration of the autologous chondrocyte Implantation procedure. (A) In a first surgery, a cartilage biopsy is taken digested, and cells cultured. (*B)* In a second surgery, a pouch is created over a debrided AC defect with a periosteal flap and the autologous chondrocyte suspension is injected in the defect. [36]. Licence number: 4655050503678.

MACI is a recent adaptation of ACI, with the difference that the chondrocytes are seeded onto a scaffold prior to being implanted into the affected site of the AC [37]. It is therefore the application of tissue engineering concepts to AC repair.

Mosaicplasty is a surgical intervention that involves the transplantation of osteochondral samples into the site of AC injury [38]. Osteochondral samples can either be obtained from the patient at non-load bearing locations or from deceased donors.

The advantages and disadvantages of each of the conservative and surgical strategies described thus far are highlighted in Figure 2.6. below.

Treatment options	Advantages	Disadvantages
Exercise	Decrease clinical symptoms, improve joint functions, prevent disability	Poor form can cause further damage
Weight loss	Reduced pain, significant improvement in function and pain if weight is lost and maintained	None
Strength training	Decreased pressure on joints, improved stability, decreased pain, improved function, slower rate of degeneration	Poor form can cause further damage
Braces	Alleviate pain, improved function, provide more stability	Uncomfortable, poor fitting, actions limiting
Oral non-steroidal anti-inflammatory drugs (NSAIDs)	Pain relief	Increased risk of gastrointestinal, renal, cardiac and vascular side effects
Topical NSAIDs	Significant reduction in pain, minimal systemic absorption	Slight increase in skin irritation
Supplements	Slight pain reduction, slight protective effects for joints (only for glucosamine),	Effects might not be significant
Prolotherapy and biologics	Promotion of fibrocartilage and hyalinelike cartilage formation in animal studies, reduced pain, improved function	Fear of needles, lack of insurance coverage
Surgical options (usually for moderate to severe degenerative joint diseases)		
Non-cell reconstruction therapies		
Mosaicplasty	Promote regeneration of fibrocartilaginous cartilage	Limited donor site, availability of donors, limited high quality graft, variable outcomes
Microfracture		Formation of post-surgical fibrocartilaginous tissues lack mechanical properties, require very long post-surgical treatment, efficacy of treatment depends largely on age and initial extent of damage, variable outcomes
Autologous chondrocyte implantation	Usage of arthroscopy minimizes damage, autologous cells minimizes rejection and prevent implantations of external pathogens	Two surgeries required, require very long post-surgical treatment, variable outcomes
Matrix-induced autologous chondrocyte implantation	Superior in-vitro histological results	No superior functional outcomes when compared to autologous chondrocyte implantation or microfracture

Figure 2.6. Table listing the advantages and disadvantages of the main OA and damaged cartilage treatment options. Licence: Hooi Yee Ng et al. [26] (open access).

2.2.2.3. Joint replacement

The cell- and tissue-based surgical interventions for AC repair are thus far only applicable for relatively small focal defects. The ultimate remedy provided when none of the above mentioned intervention are deemed to be beneficial is to perform a joint replacement were the entire affected joint is removed and replaced with metallic, metal-polymer, or metal-ceramic implants

[39]. These implants allow the patients to recover some degree of range of motion and activity level, while decreasing pain.

2.3. Drug delivery system into the joint

Ensuring the bioavailability of drugs within the joint space has been identified as a major hurdle to the development of DMOADs. Because of the absence of blood vessels in AC, the local administration of drugs has been favoured over systemic delivery strategies. Intra-articular injections allow to bypass barriers to drug transport across vascular walls and the ECM of the synovial membrane and into the synovial fluid, where the drug can diffuse through the AC layer. This strategy has consequently been associated with increased local bioavailability, reduced systemic exposure, and decreased off-target effects [40]. However, intra-articular injection is a difficult intervention that must be executed by specialists, making this drug delivery strategy costly and logistically complex. The fact that OA is a chronic condition that develops over a period of years to decades further exacerbates the situation. In addition, injected molecules are typically removed from the joint via the lymphatic system in a manner of hours, such that maintaining drug levels within their therapeutic window is often difficult in clinical settings. Efforts have therefore centered on the development of strategies to increase drug retention time within the joint following intra-articular injection, with hydrogels, microcarriers and nanoparticles being the principle approaches investigated for this purpose.

2.3.1. Nanoparticles for drug delivery into the joint.

Nanotechnology has recently gained interest in medical applications for its wide range of potential applications. Nanomaterials are materials with at least one of their external dimensions ranging between 1 and 100 nm or having internal or surface structures in the same range [40]. At that length scale, materials exhibit unique properties caused by the increased contribution of

surface molecules in relation to those in the bulk.

One type of nanomaterials, nanoparticles, are solid, colloidal particles with at least one of their dimensions ranging from 1 to 100 nm [41]. While particles with their smallest dimension above 100 nm but below 1 μm should be termed sub-micron particles, they are often also reported in the literature as nanoparticles. Due to their small size and larger surface area nanoparticles have been explored extensively for therapeutic drug delivery. Nanoparticles offer a unique opportunity for drug delivery in the joint. Beyond their size, which can be optimized for tissue infiltration, surface properties including functionalization with bioactive moieties, drug loading and releasing capacity can be tailored; however, the potential toxicity of the nanoparticles should also be monitored [90]. In a seminal paper for the field, Hubbell and colleagues proposed using the AC layer as a reservoir for therapeutic molecules and developed synthetic nano biomaterials that were small enough to penetrate the small pores of articular cartilage ECM and accumulate in its ECM and inside the cells [42] [43]. This was achieved by functionalizing the nanoparticles with a collagen type II binding peptide identified to achieve prolonged retention in the cartilage. Since this early effort, a broad range of nanocarriers have been proposed, including cationic and polyelectrolyte nanoparticles, which have exploited the Donnan effect in AC to achieve increased penetration depths and was an innovative strategy towards tissue regeneration.

2.3.2. Types of nanoparticles and fabrication techniques

Several biopolymeric [44], ceramic and synthetic polymer [45] nanoparticles have been developed for drug delivery applications. Here, a short review of the main classes of nanoparticles that have been designed for delivery into synovial joints for treating OA and other joint diseases will be discussed.

2.3.2.1. Chitosan-based particles

Wang et al., [46] utilized the ionic cross-linking property of hyaluronic acid and chitosan and produced particles with a sub-micron size of 460 nm and were subsequently delivered to OA affected knee of rats. Results obtained from the experiments carried out by this research group showed that the hyaluronic-Chitosan nanoparticles had the ability to decrease apoptosis in chondrocytes by inhibiting inflammatory mediators and the major catabolic pathways that participate in OA pathogenesis.

Inhibition of synthesis of interleukin-1β (IL1β) [85] was performed by Zhaou et al. and his research group were Hyaluronic acid-chitosan sub-micron scale particles containing plasmid DNA encoding Cytokine response modifier A (CrmA) (particles were collectively known as HA/CS-CrmA nanoparticles) were produced. The main reason behind selecting CrmA is that it naturally possesses the property of inhibiting the synthesis of IL1β. OA model of rat anterior ligament was tested with these particles which released the plasmid DNA for up to 3 weeks which thereby significantly inhibited cartilage damage, inflammation of the synovium and considerable loss of type II collagen.

Zinc is considered necessary for maintaining bone homeostasis which unfortunately decreases tremendously when affected with rheumatoid arthritis (RA). Zinc-Chitosan nanoparticles were formed using the ionic gelation method with a particle diameter of 106.5 ± 79. Treatment on RA affected rats with these nanoparticles showed reduced severity of RA [86] and also decrease in the level of biomarkers of inflammation.

2.3.2.2. Alginate

Alginate has been used to form nanoparticles for drug delivery into the joint for treating OA and RA. Such particles were used to deliver glucosamine sulfate, which is usually delivered orally

for the treatment of OA, directly to the joint [47]. The authors showed that these nanoparticles had a very high retention over 7 hours in the joint of rats. The nanoparticles could also be used for topical administration, thereby overcoming the disadvantage of oral administration.

Alginate-chitosan-Pluronic sub-micron particles [88] were formed by ionotropic gelation and were optimized for different parameters such as particle size, zeta potential, and entrapment efficiency to aid in IA delivery of NSAID's. The average particle size of the optimized particles was 283 nm. Alginate-chitosan particles were also synthesized by ionotropic gelation to deliver Methotrexate [89] were the compound is said to have anti-cancer, anti-rheumatic drug having a very high solubility and low permeability properties.

Shardool et al. encapsulated an anti-inflammatory IL-10 cytokine encoding plasmid NDA into an alginate-based nanoparticles [90] and the surface of the nano-carrier was modified with the tuftsin peptide to achieve targeted delivery. Treatment with these nanoparticles in the inflamed paws of arthritic rats resulted in significant decrease in joint tissue pro-inflammatory cytokines and also maintained the mobility of the rats up to 5 days.

2.3.2.3. Liposomes

Liposomes are spherical vesicles made of phospholipids organized in lipid bilayers and are being extensively exploited for drug delivery applications. Xiuling et al., [48] prepared glucosamine sulphate encapsulated liposomes using 1,2-distearoyl-*sn-glycero*-3-phosphocholine (DSPC), which is said o have a high retention capacity and also has the potential to down-regulate pro-inflammatory cytokines such as Tumor Necrosis Factor-α (TNF-α) and upregulate anabolic components.

Liposomes were also used to encapsulate a drug named dexamethasone said to possess antiarthritic properties. These particles were effective in inhibiting the progression of arthritis in rats affected with RA [92]. Hyaluronic acid-conjugated liposomes encapsulating prednisolone were also

developed by Virginia et al. for targeted delivery to RA affected sites in rats. The authors also showed that these particles were pH-sensitive [93] and were useful in providing targeted release to the inflamed synovial cells, which can be beneficial for treating RA.

2.3.2.4. Synthetic polymer and ceramic nanoparticles

Other base materials have also been used for the fabrication of nanoparticles to treat joint diseases. These include synthetic polymers and ceramics. For example, chitosan-graft-polyethyleneimine nanoparticles were developed by Huading et al. to act as non-gene novel vectors for gene therapy in OA [22]. The group produced these nanoparticles by initially grafting chitosan and then through a complex coacervation of the cationic polymer with polyethyleneimine. These experiments showed that these nanoparticles had higher efficiency, lower cytotoxicity such that they can be considered a safe and efficient non-viral vector for gene therapy to both the synoviocytes and chondrocytes. Also, silver nanoparticles have been bio fabricated using Caffeic acid by Qingyan Lin et al. These showed increased stability as well as improved advantages in the fields of drug delivery, bioimaging and also showed that the level of cytotoxicity of osteoarthritic chondrocytes could be controlled using these particles [82].

2.4. Inorganic polyphosphate

PolyP is a linear polymer of orthophosphate residues linked by energy-rich phosphoanhydride bonds (Figure 2.7.). The chain length of polyP molecules can vary from two to several hundred units. The polyP molecule with only two orthophosphate groups is typically referred to as inorganic pyrophosphate and has been studied a lot [74].

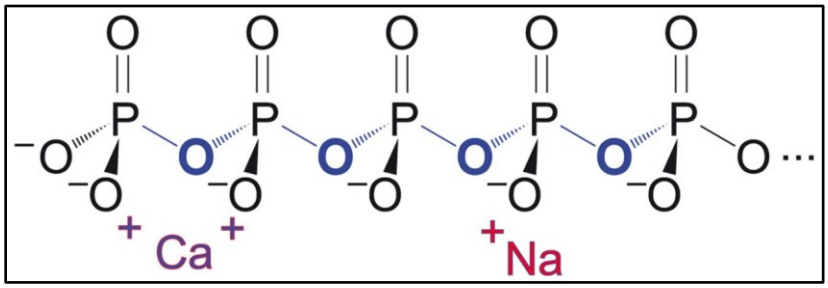

Figure 2.7. Chemical structure of inorganic polyphosphate [41]. Licence number: 4657460401383.

2.4.1. Natural occurrence of polyP

Biological polyP was first observed in yeast cells [75] and was also found in granules present in the cytoplasm of bacteria [76]. Since then polyP has been found in microorganisms of all three branches of the tree of life [73]. Importantly for this work, polyP has been observed in a number of vertebrate cells and tissues [76-80], where it found in various cell compartments.

2.4.2. Biological roles of polyP

While a relatively small number of studies have been carried out on the roles played by polyP in mammalian cells and tissues, functions in coagulation [6] [49], mineralization [6, 49], ion chelation [50], and interactions with nucleic acids and proteins [6], have been identified. These interactions have been found to stabilize biomolecules. For example, experiments involving heating of thermo-labile proteins such as luciferase in the presence of polyP demonstrated that the proteins remained stable and soluble at high temperatures [79]. Similarly, polyP was shown to bind to acidic and basic fibroblast growth factors (FGF-1 and FGF-2, respectively) [86] and enhance their effects on the proliferation of human fibroblasts modulation .Other roles include the ability of polyp to act as a source of energy and a chelator of cations because of its ability to form salts with cations including Ca^{2+},Mg^{2+} Zn^{2+}, Fe^{2+},Na^{2+},K^{+} [76].

2.4.3. Effects of polyP on cells of the joint and cartilage

St-Pierre et al. [6] were the first to demonstrate that treatment of chondrocytes, the cells of AC, led to a significant increase in ECM accumulation in the cultures. They also observed a similar effect with tissue explants. In fact, this study showed increased GAG and collagen contents in the two culture models when treated with polyp characterized by chain lengths of 5, 45 and 75 orthophosphate units where polyphosphate with average chain length of 45 units exhibited the highest increase in ECM accumulation. The DNA content of the *in vitro* formed cartilage tissues increased at a slower rate in the presence of polyP than in control conditions suggesting the inorganic polymer controlled the rate of proliferation of the chondrocytes. This result was opposite from previous literature in other cell types. An unpublished study by Dr. St-Pierre and his colleagues also demonstrated that the injection of polyP in the knees of meniscectomized guinea pigs twice a week led to decreased signs of OA at two months post meniscectomy. Taken together, these two studies suggest that polyP has potential for use in cartilage tissue engineering and as a DMOAD candidate. Although work remains in order to establish the mechanisms of action of polyP on the cells of the joint. Another study by St-Pierre et al. showed that exogenous administration of polyP reversibly inhibits the mineralization process in cartilage [6]. This result is also important in the context of joint diseases because ectopic mineralization is associated with the pathogenesis of OA.

2.5. PolyP particles

PolyP is a polyanionic molecule and can therefore bind reversibly with cations via ionic bonds [51]. This property has been exploited by a number of groups to synthesize polyP particles. For example, Donovan et al. employed a precipitation approach to form sub-micron particles of polyP in a solution containing calcium and magnesium [51]. Others were able to incorporate

different cations into the particles from strontium, to magnesium and aluminum [51]. The addition of these cations can serve to provide additional bioactivities to the resulting particles. Similarly, these particles have been loaded with other bioactive molecules such as retinol for delivery to cells [52]. Interestingly, Gabriella et al. formed electrostatic complexes between guanidium-rich oligocarbonate transporters and polyP' to form discrete nanoparticles that are resistant to phosphatase enzymes. These particles can be internalized into multiple cell types [91]. These studies provide a template for the development of our protocol for the synthesis of polyP nanoparticles; however, relatively little work has been carried out so far to fully understand the effect of synthesis parameters on particle size, surface charge and stability.

CHAPTER 3 – MATERIALS AND METHODS

3.1. Materials

The cell culture medium Dulbecco's Modified Eagle Medium (DMEM) with glucose and the fetal bovine serum (FBS) were purchased from Corning cellgro, the penicillin-streptomycin solution, Triton X-100 and Dimethyl sulfoxide were from Sigma Aldrich, the enzymes used for the tissue digestion, pronase and collagenase type I from *Clostridium histolyticum* were purchased from EMD Millipore corp and Alfa Aesar, respectively. Chloramine-T was also from Alfa Aesar. All assay kits were purchased from Thermo Fisher Scientific. All tissue culture plastic, as well as Trypsin, IL1β, Bovine Serum Albumin (BSA), L-ascorbic acid, citric acid and PBS were purchased from VWR. Proteinase K was purchased from R&D systems, EDTA, acetic acid, hydrochloric acid, and Tris HCl for Molecular Biology, and nitric acid was from Fisher Scientific. Calcium chloride was purchased from ACP, sodium chloride from I-chem and 4-dimethyl amino benzaldehyde from Acros Organic. Sodium polyphosphate was a kind gift from Budenheim.

3.2. Effects of polyP on FLS cell

3.2.1. FLS cells isolation and seeding

Bovine FLS cells were isolated by excising the synovium from the phalangeal-metacarpal joint of cow legs purchased from a local abattoir (Tom Henderson Meats & Abattoir). The legs were washed, soaked in 70% ethanol for 30 minutes and carefully dissected in a biosafety cabinet to minimize the risks of contamination. The excised synovium was digested by incubation with a 1% pronase solution in DMEM with 1% penicillin-streptomycin solution for 1 hour, 3 washing steps in phosphate-buffered saline (PBS), and incubation with 0.2% collagenase type I Clostridium histolyticum in DMEM with 1% penicillin-streptomycin solution for 24 hours at

37˚C in 100% humidity and with 5% CO_2. The digested tissue solution was strained (100 μm pore-size strainers) and centrifuged at 300 rcf for 3 minutes. The cell pellet was resuspended in DMEM supplemented with 10% FBS and 1% penicillin-streptomycin, seeded in T175 flasks at a cell seeding density of 5714.29~~13.57~~ cells/cm^2 and incubated at 37˚C in 100% humidity and with 5% CO_2. Once cells reached approximately 90% confluence, they were passaged. For this process, the cell monolayer was washed in DMEM (without FBS) and detached with Trypsin-EDTA. The reaction was stopped by addition of FBS. These cells were centrifuged, the supernatant removed and replaced with fresh DMEM. The process was repeated 2 more times and the cells were resuspended in supplemented DMEM, before seeding in new T175 flasks or cryopreserved in DMEM with 10% FBS and 10% dimethyl sulfoxide by controlled freezing to -80°C. FLS cells at passage 2 to 6 were used for all further experiments.

For experiments, FLS cells were counted using a hemocytometer and, unless specified otherwise, seeded at 1,250 cells/cm^2 in treated 24 or 48 well plates (depending on the experiment) in 1 mL of supplemented DMEM. The seeding step will be referred to as day (-1) throughout the thesis. Cells were allowed to attach to the wells for 24 hours before the medium was changed to the treatment conditions. This medium change to incorporate polyP with the culture medium of select cultures will be referred to as day 0 and all studies were performed at days 1, 3 and 5 from that treatment initiation. For polyP treatment, DMEM supplemented with 10% FBS and 1% penicillin-streptomycin was prepared with varying concentrations of the inorganic polymer ranging from 0 to 5 mM calculated on a phosphate basis (rather than a polymer basis; this is the standard approach in the field). It should be noted that concentrations of polyp 1mM and higher led to precipitation following incubation with cells. The media were changed every 48 hours. Figure 3.1 illustrates the cell isolation and seeding protocol.

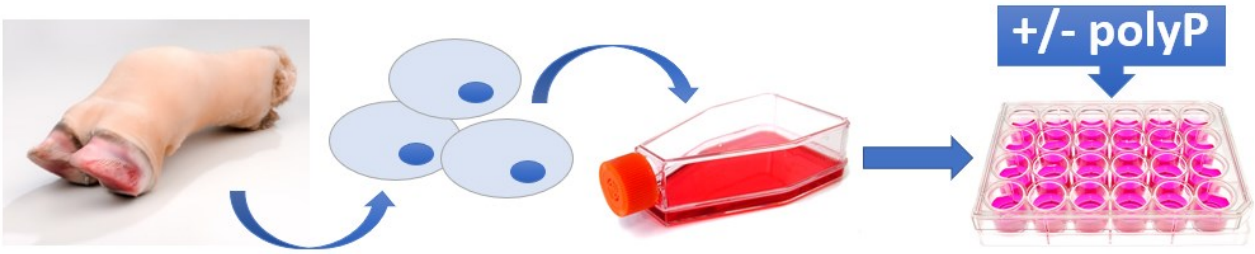

Figure 3.1. Schematic of the FLS cells dissection and seeding process.

3.2.2. Cell morphology

FLS morphology was assessed at different time points (1, 3, and 5 days) following incubation in the presence and absence of polyP by staining with the phalloidin dye, which binds the actin filaments inside the cell cytoplasm. Cells were washed in PBS, then fixed in 3.7% formaldehyde in PBS for 15 minutes. Cells were then permeabilized in 0.1% Triton X-100 in PBS for 3 minutes and washed in PBS 3 times. Blocking was achieved by incubation with 3% w/v bovine serum albumin (BSA) in PBS for 1 hour. Cells were then incubated with 2 μM Alexa Fluor™ 488 Phalloidin in PBS for 15 minutes, washed 3 times PBS and counterstained with nuclear dye 4′,6-diamidino-2-phenylindole (DAPI; 1 mg/mL) for 5 minutes. Cells were washed 3 times in PBS and imaged with an epifluorescence Olympus 1X81 microscope with a Q-Imaging Retiga Exi Fast 1394 series camera using the FITC and DAPI filters. Six images were taken at randomly selected positions in the wells for each sample. All steps were carried out at room temperature.

3.2.3. DNA quantification

The DNA content of cultures at different time points and in the presence of different polyP concentrations was measure using the Quant-iT Pico Green dsDNA assay to provide an estimate of the number of cells in each sample. This assay was performed according to the protocol obtained from Thermo Fisher Scientific, with minor changes to the volumes used. Briefly, samples were digested with a 0.2 mg/ml proteinase K solution in digestion buffer (0.1 M sodium

chloride, 10 mM Tris hydrochloride, 1 mM ethylenediaminetetraacetic acid (EDTA), 0.5 %v/v SDS, pH 8.0). The digest was frozen at -20˚C until used. A 25 μL aliquot of the digest was diluted with 25 μL of TE buffer and mixed with an equal volume of Pico Green solution in TE buffer. A standard curve was generated with Lambda DNA diluted serially in TE buffer. Solution fluorescence was measured using a Tecan Infinity M1000 spectrofluorometer at excitation and emission wavelengths of 480 and 520 nm, respectively.

3.2.4. Proliferation assay

The percentage of FLS that were actively proliferating within a given period were evaluated using the Click-iT Plus EdU Imaging kit according to the instructions provided by Thermo Fisher Scientific with minor changes to the volume used. The chemical 5-ethynyl-2'-deoxyuridine (EdU) is a thymidine analog that is incorporated into newly synthesized DNA during proliferation. Its incorporation in DNA can be detected via a copper catalyzed click reaction between a picolyl azide(contained in the Alexa Fluor dye) and an alkyne. The assay is performed by adding 2 μL of 10 mM EdU stock solution per mL of fresh supplemented DMEM and incubating the cells at 37˚C in 100% humidity and 5% CO_2 for 4 hours. The cells were then washed in PBS and fixed with 3.7% formaldehyde in PBS at room temperature for 15 minutes. The cells were then incubated twice with 3% BSA in PBS for 15 minutes at room temperature to block unspecific binding of the dye. Samples were then permeabilized with 0.5% Triton X-100 at room temperature for 5 minutes. The permeabilization solution was removed and the cells were washed twice with 3% BSA in PBS, followed by 30 minutes incubation with a solution made of Click-iT EdU reaction buffer, copper sulphate solution, Alexa Fluor^{TM} 488 dye and Click-iT buffer additive according to supplier provided concentrations. This step was performed protected from light at room temperature. Wells were washed again with 3% BSA, followed by incubation

with of Hoechst dye (33342) for 15 minutes at room temperature and subsequently washed PBS. Samples were imaged under a fluorescence epifluorescence Olympus 1X81 microscope with a camera from Q-Imaging Retiga Exi Fast 1394 series using the FITC and DAPI filters. Six images were taken at randomly selected positions in the wells for each sample. The total number of cells and the number of proliferating cells in each image were counted manually and the percentage of proliferating cells was determined by dividing the number of EdU stained cells by the total number of cells stained with DAPI a minimum of 45 cells were counted for each condition. Images were also overlapped using ImageJ software.

3.2.5. Live/Dead Viability test

The Live/Dead cytotoxicity and viability kit was purchased from Thermo Fisher Scientific and the assay was performed according to the instructions provided by supplier Thermo Fisher Scientific with minor changes to the volumes used. This assay allowed to evaluate the potential for cytotoxic effects of polyP on FLS cells. Briefly, cells were washed with PBS and incubated with 4 mM Calcein AM and 2 mM Ethidium homodimer-I in DMEM supplemented with FBS and penicillin-streptomycin and incubated for 20 minutes at 37˚C in 100% humidity and 5% CO_2. Cells were then washed in supplemented DMEM and imaged with an epifluorescence Olympus 1X81 microscope with a camera from Q-Imaging Retiga Exi Fast 1394 series. Live and dead cells were imaged with the FITC and TRITC filters, respectively. Six images were taken at randomly selected positions in the wells for each sample. The number of live (green fluorescence) and dead (red fluorescence) cells were counted manually.

3.2.6. MTT metabolic activity assay

The metabolic activity of FLS cells was assessed using an MTT Cell Proliferation Assay kit from Thermo Fisher Scientific according to the instructions provided by the supplier with minor

changes to the volumes used. This was of interest to us because polyP is a molecule with energy rich phosphoanhydride bonds between orthophosphate groups. This assay involves the conversion of the water soluble compound 3-(4,5-dimethylthiazol-2-yl)-2,5-diphenyltetrazolium bromide (MTT) to an insoluble formazan that can then be solubilized using sodium dodecyl solution (SDS),and quantified based on optical density. The assay was initiated by removing the culture medium from all the wells with cells and three wells without cells (controls) and replacing it with 150 μL of fresh DMEM with 10% FBS and 1% penicillin-streptomycin with 15 μL of the MTT solution prepared in PBS, before incubating at 37˚C in 100% humidity and 5% CO_2 for 4 hours. A 150 μL volume of SDS in 0.01M HCl was then added and incubated for 20 hours to dissolve the crystals. Aliquots were then read spectrophotometrically at 570 nm using an Epoch plate reader from BioTek. Background optical density measured from the controls (without cells) was subtracted from the optical density for each sample.

3.2.7. 2D Cell migration test

Cell migration was assessed in 2D using a scratch test. Briefly, FLS were seeded into 24 well plates and allowed to reach confluence. Cells were then cultured with or without 2.5 mM inorganic polyphosphate for 24 hours before a scratch was made on the surface of each well with a 10 μL pipette tip. At different time points from 0 to 24 hours, images of the scratch were taken to allow measurements of its width using ImageJ (U.S. National Institutes of Health). Ten measurements were taken for each sample at equal spacing from the previous measurement and averaged for each time point.

3.2.8. Interleukin-1β treatment of FLS cells

Interleukin-1β (IL1β) treatment is often used to simulate OA-associated inflammation *in vitro*. FLS cells were treated with IL1β from R&D systems and reconstituted according to the supplier

instructions (at 10 ng/mL in 0.1% BSA in PBS) up to day 5 to attempt to stimulate proliferation, nitric oxide (NO) and collagen production assessed by DNA quantification, a total NO assay and a collagen assay. Treatment concentrations investigated were 1 and 10 ng/mL as per previous studies in the literature [87].

3.2.9. Total NO content

NO is a signaling molecule that plays an important role in the pathogenesis of OA as a pro-inflammatory mediator. The effect of polyP on the production of NO by FLS cells was investigated. Cells were cultured (100,000 cells/well) for 24 hours. Conditioned medium was obtained and frozen immediately on dry ice and stored at -80˚C until testing. The total NO assay was performed using a kit from Thermo Fisher Scientific according to the instructions provided by the supplier with minor changes to the volumes used. Briefly, conditioned medium was diluted with equal volumes of reagent diluent and 12.5 μL each of NADH and nitrate reductase. The plate was sealed and incubated for 30 minutes at 37˚C. Two volumes of each of the Griess reagents I and II were then added and samples incubated at room temperature for 10 minutes. Standards were prepared with nitrate. The plate was then read spectrophotometrically using an Epoch plate reader from BioTek at an absorbance of 560 nm.

3.2.10. Collagen content

Collagen content deposited by FLS cells was estimated with an hydroxyproline assay. Cells were cultured at 100,000 cells per well for 3 days. The samples were then digested with proteinase K as described previously. An aliquot of the digest was mixed with an equal volume of 6N hydrogen chloride and heated at 110˚C for 18 hours to hydrolyze the proteins in the sample. The hydrolyzate was neutralized by adding a volume equal to the sample aliquot of 5.7N sodium hydroxide. Samples were diluted to appropriate concentrations using distilled water based on

previous work to ensure that the diluted sample concentration would fall within the linear portion of the standard curve. An aliquot of 120 μL was mixed with a half volume of 0.05N chloramine-T in 20 %vol distilled water and 30 %vol methyl-cellosolve and 50 %vol hydroxyproline buffer (pH 6.0, see Table 3.I.) and allowed to react for 20 minutes to convert hydroxyproline to a pyrrole, followed by the addition of a half volume of 3.15N perchloric acid, with incubation at room temperature for 5 minutes and the subsequent addition of a half volume of 0.2 g/mL Ehrlich's reagent in methyl-cellosolve, which was allowed to react with the pyrrole at 60˚C for 20 minutes. Samples were then cooled in an ice-cold water. Absorbance was measured spectrophotometrically at 560 nm using a Epoch plate reader. Standards were prepared by serial dilution with trans 4-Hydroxy-L-proline. Collagen content was estimated by multiplying hydroxyproline content by a factor of 10, because hydroxyproline has been estimated to represent approximately 10% of amino acids in collagen type II.

Table 3.I. Composition of the hydroxyproline buffer.

COMPONENT	**COMPOSITION**
Citric acid	0.5 g
Glacial acetic acid	120 uL
Sodium acetate	723 mg
Sodium hydroxide	340 mg

3.3. Calcium-polyphosphate particles

3.3.1. Calcium-polyP particle synthesis

Calcium-polyP particles were prepared in a 100 mL beaker with a rotating magnetic stir bar of dimensions 8x22 mm with orthogonal sides agitated with a magnetic stir plate by drop-wise addition of a polyP solution in 8mM Tris buffer with varying concentrations of sodium chloride

(pH was adjusted upon addition of polyP to the buffer; different pH were investigated from 4.0 to 10.0 based on conflicting reports from literature) into a calcium chloride solution in the same buffer. The experimental set-up is illustrated in Figure 3.2. A number of synthesis parameters were controlled and operated at different values during the synthesis process to gain insight into their effects of particle size. These included the mixing rate (200-800 rpm) and the inlet drop rate (0.5-1.5 mL/min) for the addition of polyphosphate, concentrations, and pH. Details of the ranges investigated are provided in Table 3.II. These ranges were selected based on previous work in the literature and preliminary studies in the lab. After the addition of the polyP solution into the calcium chloride solution, mixing was continued for 24 hours. Selected experiments involved the addition of different concentrations of trisodium citrate dihydrate at different stages in the process. Details of these experiments will be provided in the description of results. This addition was intended to stabilize the particles following issues with stability.

Table 3.II. Value ranges investigated for the calcium-polyphosphate synthesis.

Parameter	**Varying range**
Mixing rate	200-800 rpm
NaCl concentration (Ionic strength)	25-75 mM
pH	4-10
$CaCl_2$	4-6 mM
polyphosphate concentration	4-6 mM
Drop rate	0.5-1.5 mL/min

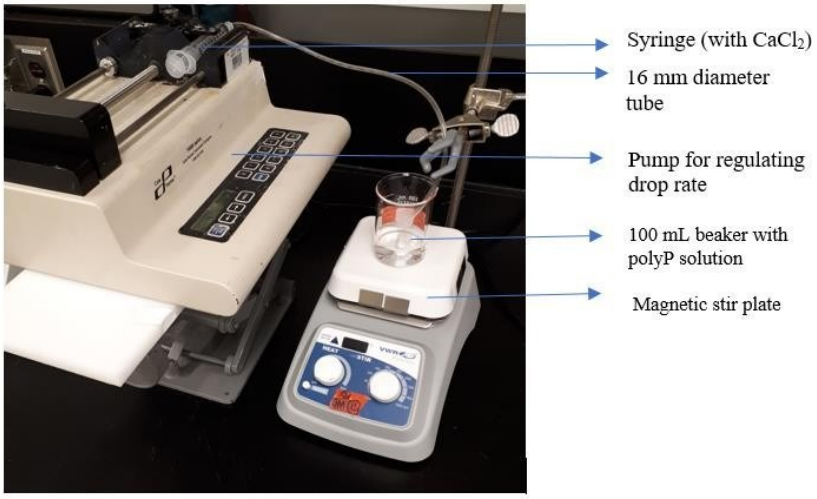

Figure 3.2. Experimental setup for the synthesis of calcium-polyphosphate particles by dropwise addition.

3.3.2. Dynamic light scattering

Average particle size, z-average and polydispersity index for each calcium-polyP synthesis were measured by dynamic light scattering (DLS) using a Nano-ZS Zetasizer. Briefly, 1 mL of the synthesized calcium-polyP particle solution was transferred into disposable plastic cuvettes purchased form Malvern and measured using a pre-set measurement file which was kept as a constant measurement file for all readings with the nature of the sample was chosen to be nanoparticle suspension with refractive index of 1.590 and adsorption set to 0.010. The dispersant was chosen to be water with temperature of 25˚C, viscosity 0.8872 cP and refractive index of the dispersant to be 1.330. The equilibrium time (in seconds) for the particles was set to 120 seconds (with 9 runs for each measurement) with cell type used as DTS 0012 cuvettes (purchased from Malvern). The optimum positioning was selected for the measurements with general purpose-normal resolution for all measurements. The parameters that were selected to be

measured every run were the size (nm) as a function of Intensity, count rate and PDI.

3.3.3. Scanning electron microscopy

Particle solutions were dialyzed for 48 hours against via a magnetic stir bar rotating at 50 rpm with change of water roughly every 4 hours. The dialysis membrane cut-off was 12-14 kDa. A 20 uL aliquot was spotted on conductive tape glued to a specimen stage and imaged with a Phenom Pro scanning electron microscope. Five images were taken per sample.

3.3.4. Particle stability

Synthesized particles were kept undisturbed at room temperature and evaluated every 24 hours with the DLS to monitor changes in the average size, z-average, and polydispersity index that may indicate agglomeration and/or dissolution of the particles.

3.4. Statistical Analysis

All experiments involving bovine FLS cells were repeated 3 times with cells isolated from 3 different animals unless specified otherwise. For each experiment, conditions were performed in triplicates unless specified otherwise. The results are expressed as means ± standard error and were analyzed using a one-way ANOVA (for more than 2 conditions) with Tukey's Post hoc test. P values ≤ 0.05 were considered to be statistically significant.

All experiments involving synthesis of the Ca-polyP sub-micron particles were repeated 3 times unless otherwise specified. The results obtained are expressed as means ± standard error and were analyzed using a one-way ANOVA (for more than 2 conditions) with Tukey's Post hoc test. P values ≤ 0.05 were considered to be statistically significant.

CHAPTER 4 – RESULTS AND DISCUSSION

Effects of polyP on fibroblast-like synoviocyte (FLS) cells

The first objective of this thesis was to study the effects of polyP on FLS cells processes *in vitro*. FLS cells are one of the two main cell types in the synovium, the thin membrane than encapsulates our joints. They are important cells in the modulation of joint homeostasis and in OA development. This chapter will present the results obtained towards this objective.

4.1. FLS cell morphology

As a first step, the effect of polyP on FLS cell morphology was investigated using a phalloidin staining. Based on Phalloidin staining, no obvious change was observed in FLS cell morphology due to treatment with polyP (Figure 4.1.). However, a greater number of cells was typically observed per frame in the non-polyP treated samples compared to the polyP treated condition at day 5. This observation suggested that polyP may have an impact on the change in FLS cell number per cultures over time, either by decreasing cell proliferation or through cytotoxic effects. This observation guided our subsequent experimental direction. Indeed, we felt that it was important to first verify these qualitative observations with quantitative data on cell number through DNA content analysis, and secondly, to determine if this decreased cell number in presence of polyP was caused by decreased cell proliferation or increased cell death.

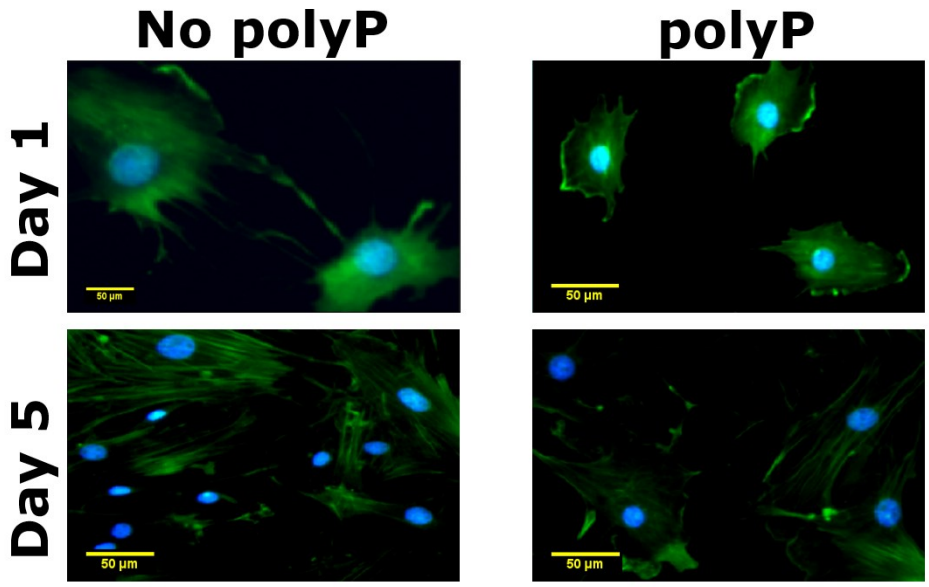

Figure 4.1. Phalloidin staining (green) of FLS cells incubated in absence or presence of polyP for up to 5 days. DAPI (blue) was used as a nuclear counterstain.

4.2. FLS cell number

Changes in FLS cell number in each culture were evaluated by quantifying the DNA content in each well. DNA content is an indirect method to estimate cell number because non-dividing cells contain the same amount of DNA. Cells were incubated with a range of polyP concentrations from 0 mM (control) to 5 mM and DNA content was measured at days 0, 1, 3 and 5. Figure 4.2. shows that treatment with polyP leads to a concentration-dependent decrease in DNA content in the cultures at day 5. This decrease was significantly different for all concentrations above 0.25 mM compared to the control. These results confirm observations from the cell morphology experiments. It must also be noted that the DNA levels increase significantly between days 1 and 5 for all polyP concentrations investigated, indicating that the FLS cells numbers are still increasing to some extent in each condition, even when a decrease in cell number compared to untreated cells was observed. These results suggest that polyp may be acting on proliferation rather than being cytotoxic to FLS cells, although this suggestion must be investigated further.

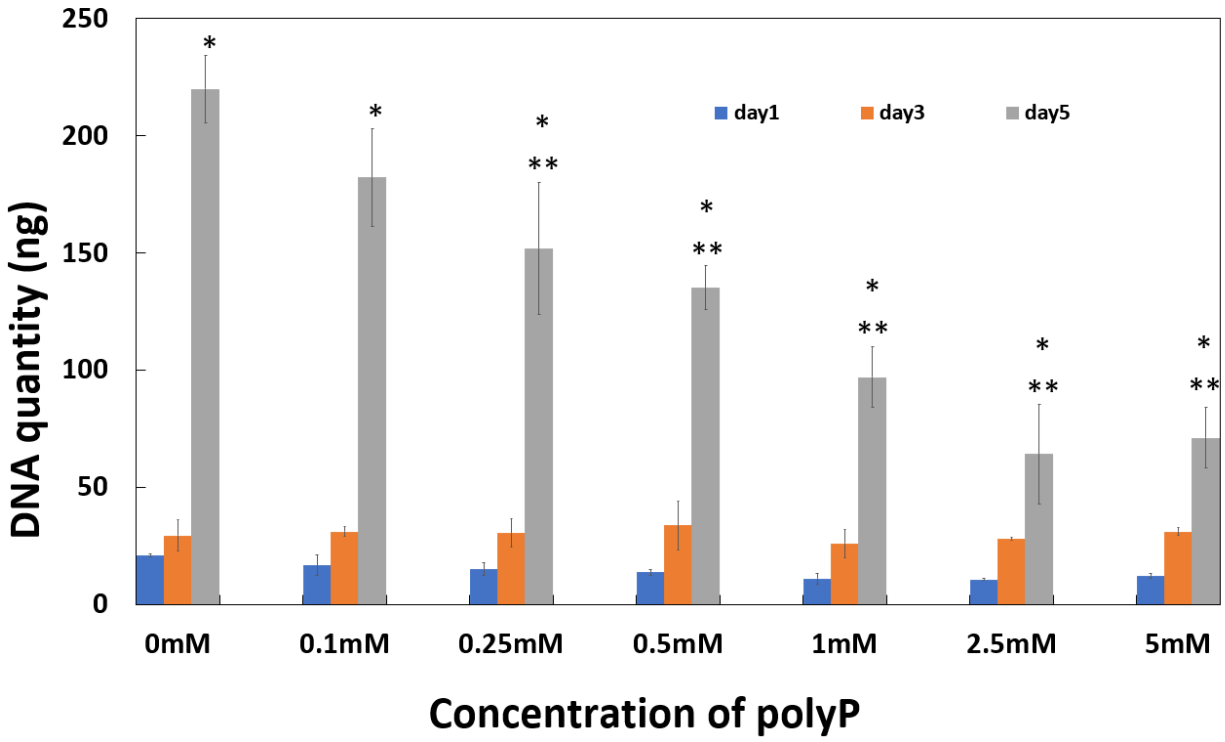

Figure 4.2. DNA content in FLS cell cultures incubated with different concentrations of polyP for up to 5 days. The experiment was performed in triplicates and repeated 3 times with cells from different animals. Data is presented as means ± standard deviation (* and ** indicates that $p < 0.05$; n=9 from 3 independent experiments).* indicates a statistically significant increase in DNA content compared to a 1 day incubation at a given polyp concentration. ** indicates a statistically significant decrease in DNA content between compared to untreated controls.

4.3. FLS cell proliferation

The number of actively proliferating FLS cells was assessed using an EdU assay, whereby EdU is incorporated into newly synthesized DNA during proliferation. FLS cells were incubated with 0, 0.25, and 2.5 mM polyP for 1 day, then incubated with EdU for 4 hours so that any actively proliferating cell during that 4 hours window would be labelled with EdU (reddish-pink fluorescence). As can be seen in Figure 4.3., a lower percentage of cells treated with 2.5 mM polyP were actively proliferating during the experimental window than in samples treated with a low concentration of polyP or in absence of polyP. This data confirms that the decreased DNA

content observed above is at least partially caused by a decreased proliferation rate in the presence of polyP. This inhibitory effect of polyp on FLS cell proliferation is in agreement with a previous observation on the effects of polyp on chondrocytes [6], but an opposite effect to that observed for human fibroblasts [86].

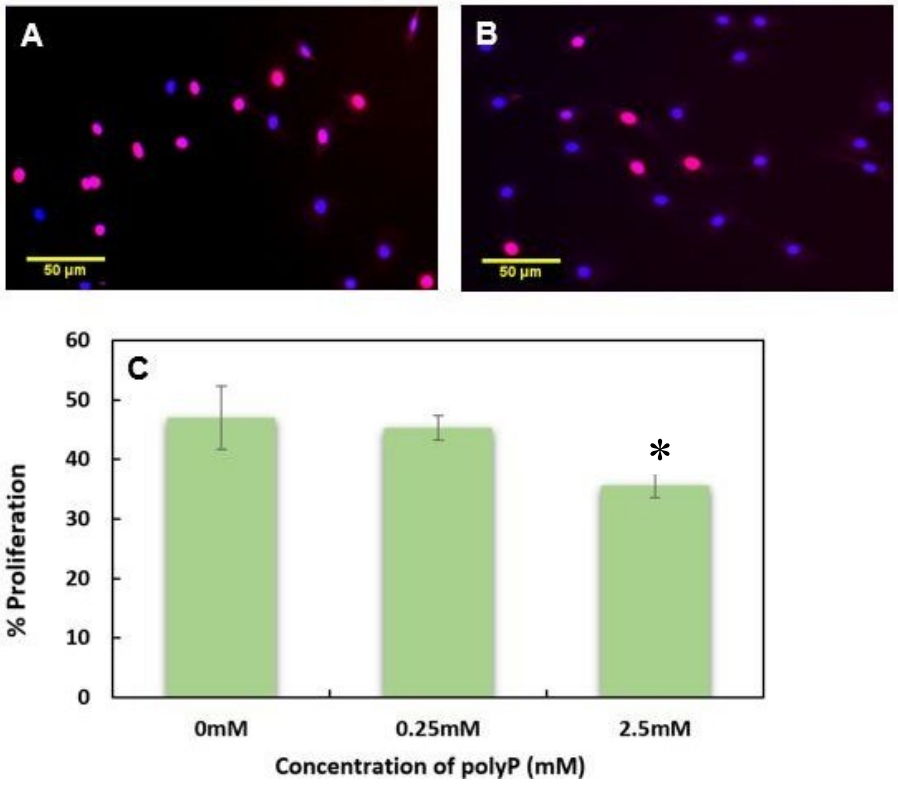

Figure 4.3. *(*A-B) Actively proliferating FLS cells identified by incorporation of EdU within newly synthesized DNA (pink; DAPI nuclear counterstain appears blue) for cells cultured (A) in absence of polyP or (B) in the presence of 2.5 mM polyP. (C) Percentage of the total number of cells counted for each condition that were EdU positive. Data in (C) presented as means ± standard deviations ($p<0.05$; n=9 from 3 independent experiments). * indicates a statistically significant difference compared to the control.

4.4. PolyP cytotoxicity on FLS cells

To establish if polyP also had cytotoxic effects on FLS cells, a live/dead staining was performed on cells treated with polyP or left untreated for up to 5 days. The concentration of 2.5 mM polyP

was selected for this test because it represented the concentration tested with the lowest DNA content at day 5. As can be seen in Figure 4.4., most cells were alive (Calcein-AM: green fluorescence) and very few dead cells (EthD-1: red fluorescence) could be observed. There was no appreciable difference between treated and untreated cells. A 70% (v/v) ethanol treatment for 5 minutes was performed as a control for dead cells and is shown in Figure 4.4.E. This result supports the idea that polyP does not elicit cytotoxic effects on the FLS cells at the concentrations tested. It also suggests that the decrease in DNA content observed in our cultures was due primarily to the inhibiting action of polyP on the rate of proliferation. Nevertheless, it cannot be excluded that the low count of dead cells may be the result of these cells detaching from the tissue culture plastic. Further work will be required to rule out this possibility.

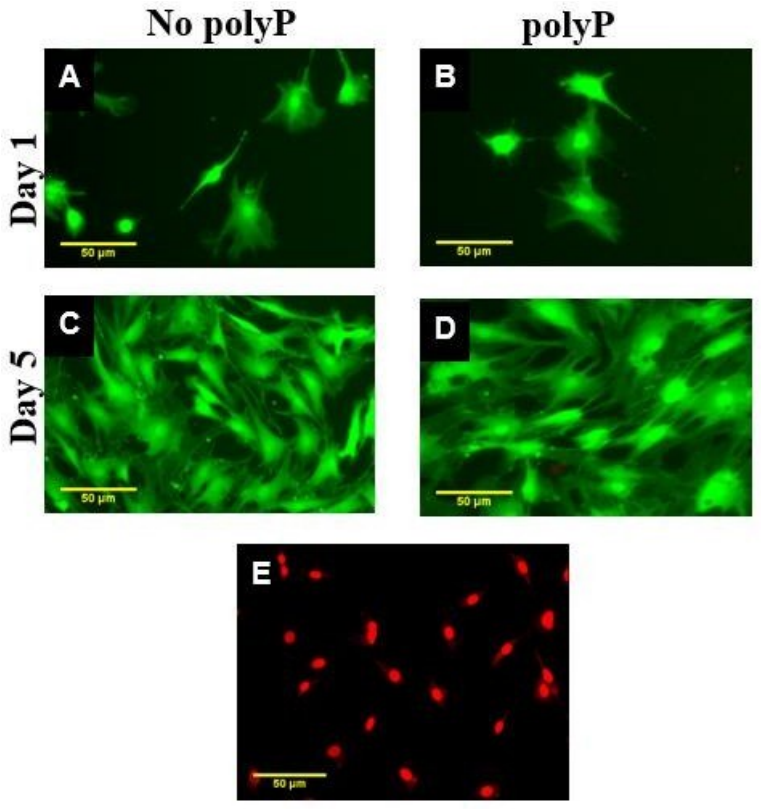

Figure 4.4. Live (green) and dead (red) FLS cells in samples cultured for (A-B) 1 or (C-D) 5 days, (A, C) in absence or (B, D) presence of 2.5 mM polyP. (E) FLS cells incubated in 70%

(v/v) ethanol prior to incubating with dyes (positive control for dead cells).

4.5. Metabolic activity

The bonds between orthophosphate groups in polyP are the same energy-rich phosphoanhydride bonds as are found in ATP, the energy currency of cells. Others have identified a role for polyP in providing an energy source/storage for cells [41]. Therefore, we investigated the effects of polyP on FLS cells metabolic activity using an MTT assay. Because we were interested in the average metabolic activity of each cell, we normalized the results to DNA content. Cells were cultured in the presence of polyP at concentrations ranging from 0 to 5 mM up to 5 days. Figure 4.5. shows an increase in metabolic activity with increasing polyP concentration at day 1, as was anticipated. This increase was statistically significant for 1.0 and 2.5 mM polyP compared to the untreated control. However, the reverse trend was observed by day 3 and decreased metabolic activity levels with no significant difference between treatment concentrations was observed by day 5. The large error bars for day 3 suggest issues with reproducibility that will need to be revisited. While it remains unclear what caused the loss of the effect from days 1 to 5, one can speculate to an adaptation by cells to the presence of high amounts of energy molecules for a prolonged period of time. A full understanding of these results will require further studies.

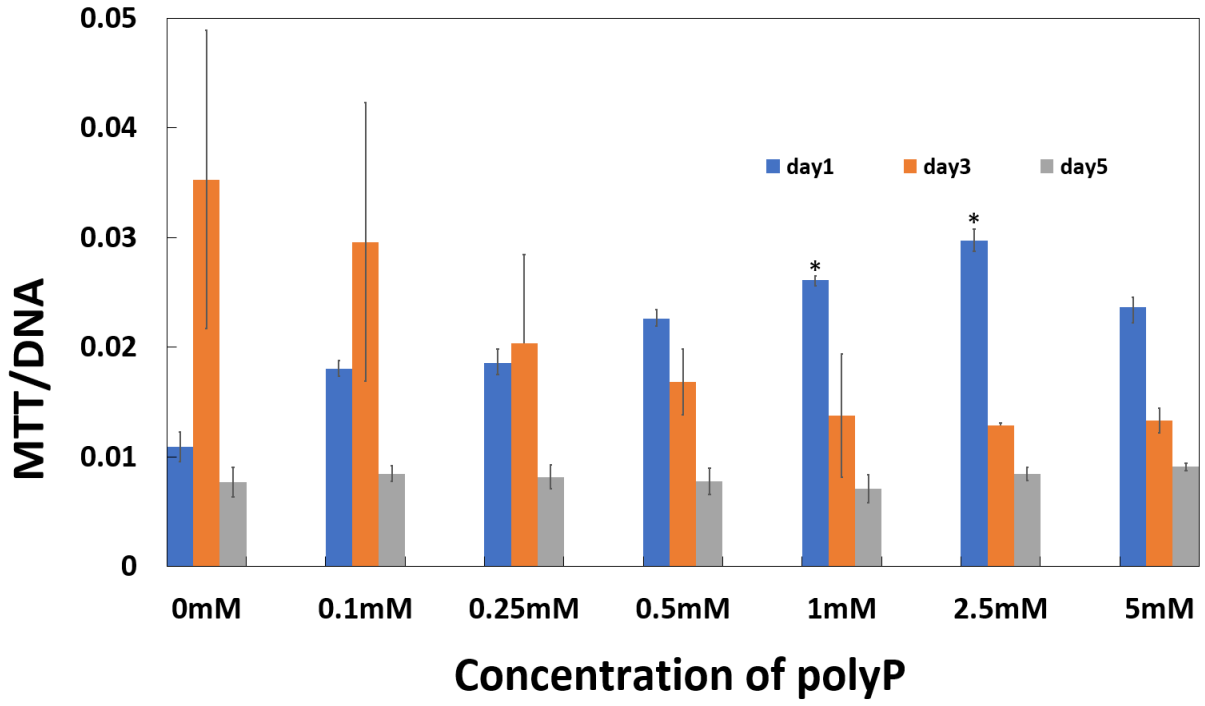

Figure 4.5. Metabolic activity of FLS cells incubated with different concentrations of polyP for up to 5 days and normalized to DNA content. The experiment was performed in triplicates and repeated 3 times with cells from different animals. Data is presented as means ± standard deviation ($p<0.05$ $n=9$ from 3 independent experiments). * indicates significant difference in normalized metabolic activity compared to the control at the same time point.

4.6. FLS cell migration

The two dimensional migration of FLS cells incubated in absence or presence of polyP for 24 hours before the experiment was determined with a scratch test. Scratch width was evaluated at 0, 3, 6, 9, 12, and 24 hours. As can be seen in Figure 4.6., cells that were first incubated with polyP migrated at a faster rate across the scratch than the cells that were not treated with polyP. By 24 hours, the gap was completely bridged by FLS cells in both conditions. This was unexpected because increased migration potential of FLS has been associated with inflammation and disease. However, it is possible that this result is a reflection of the increased metabolic activity observed after 1 day in presence of polyP.

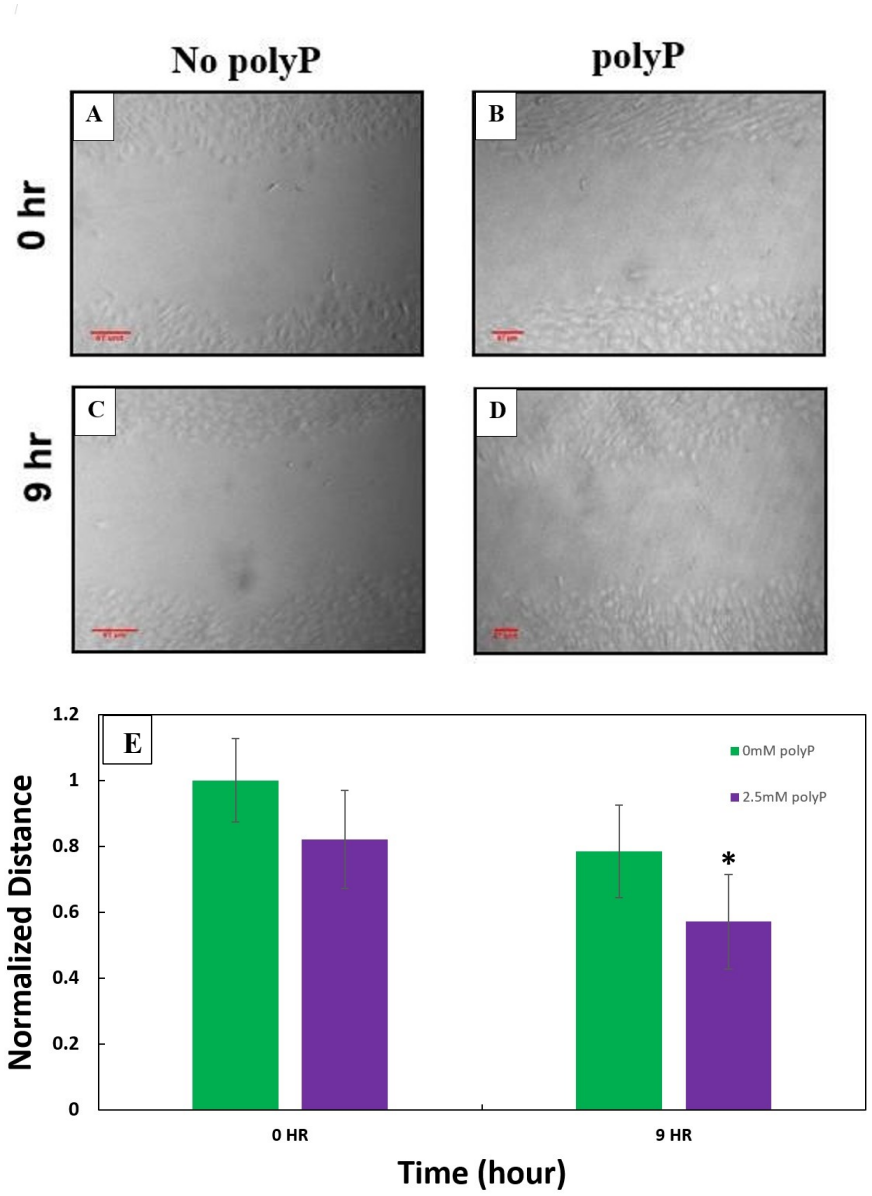

Figure 4.6. (A-D)(Above) Light microscopy images of the scratch in FLS cell monolayers (A-B) immediately after making the scratch (C-D) and 9 hours after the formation of the scratch in samples that were (A, C) untreated and (B, D) treated with 2.5 mM polyP prior. (E) Gap length change for each condition at 0 and 9 hours after the scratch was made. Data is presented as means ± standard deviation ($p<0.05$, n=30 measures from 3 independent experiments). * indicates significant difference in DNA content between different days and concentrations.

4.7. Total NO levels

The total NO content was measured in the supernatant of cells cultured in the presence or

absence of 1 and 10 ng/mL of IL1β and did not show any differences variations between conditions or with and without polyP treatment (data not shown). This was unexpected as others have shown an effect of IL1β can cause increased NO release in FLS [87]. After attempting to reproduce these results with IL1β from two different sources, this line of experimentation was stopped.

4.8. Collagen content

Hydroxyproline assay was also conducted on cell monolayers that were subject to the action of 10 ng/mL IL1β in order to increase the content of collagen deposited in our samples and examine the effect of polyP on collagen accumulation. Our results (Figure 4.7) showed that there was no significant difference in the content of collagen between our groups. These results were attributed to our inability to elicit an effect of IL1β on FLS cells. Owing to recurring issues with this model of inflammation in our hands, this line of experimentation was stopped as well.

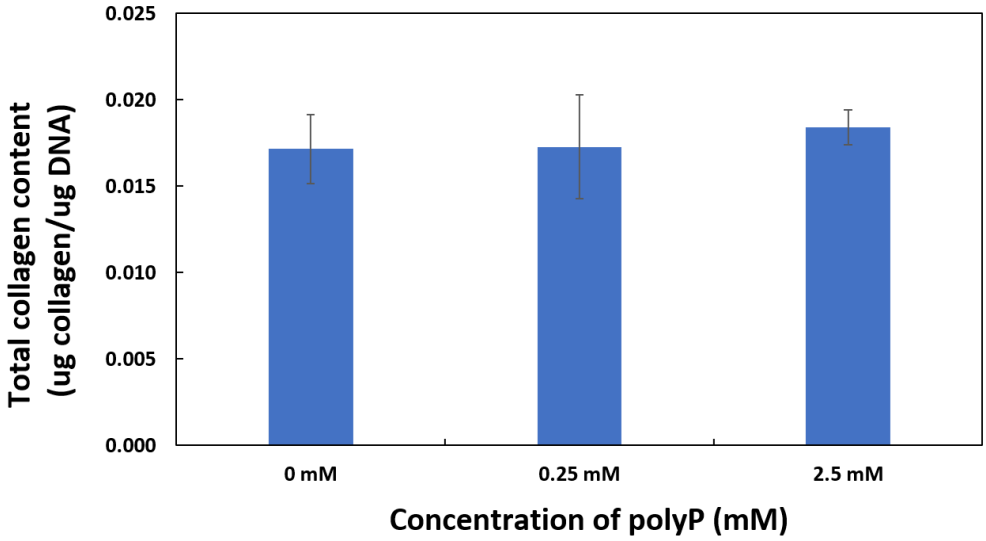

Figure 4.7. Hydroxyproline assay performed in presence of 10 ng/mLIL-1β showing no effect of polyP on collagen content. Data is presented as means ± standard deviation ($p>0.05$, n=3 independent experiments). No statistically significant difference was observed.

4.9. Summary

The studies described in this chapter demonstrate that exogenous polyp treatment does impact FLS cells processes. Of importance, our results based on fluorescence microscopy, DNA content and EdU incorporation demonstrate that polyp inhibits the proliferation of FLS cells. This is a particularly interesting finding because FLS proliferation is associated with the progression of OA [1]. Effective polyP concentrations in inhibiting proliferation were not associated with cytotoxic effects as determined by live/dead staining. However, the rate of migration of FLS cells was higher for cultures subjected to polyP treatment prior to the experiment. This was unexpected as a increased migration rate is typically associated with OA [1]. This effect on migration should be investigated further. For example, migration rate should be evaluated after longer incubations with polyP. Indeed, our results suggest that FLS cells have a higher metabolic activity in response to polyp after 1 day, but this effect may be lost after longer polyp treatments. The migration results may simply be the consequence of increased metabolic activity in the first 24 hours following treatment with polyp. However, the apparent increased metabolic activity, albeit with important reproducibility issues) in the negative control at day 3, lead us to be cautious in our interpretation of these results. Further, FLS migration in a 3D model more reminiscent of the *in vivo* environment than the 2D culture should be explored. A lack of response of FLS cells to IL1β in this study has limited our ability to push these studies further. This issue will need to be resolved in order to pursue this study further.

CHAPTER 5 – RESULTS AND DISCUSSION

Synthesis of sub-micron calcium-polyP particles

The second major objective of this thesis involved the development of a protocol to synthesize sub-micron sized calcium-polyP particles that could be used for the therapeutic delivery of polyP into the joint via intra-articular injections. Ultimately, our goal would be to ensure retention into the AC tissue via functionalization of the particles with molecules that elicit specific binding to AC ECM molecules; however, efforts for this thesis were limited to achieving the synthesis of stable particles and investigating our ability to control their size. This chapter will present the results obtained towards this objective.

5.1. Challenges faced during the development of the synthesis protocol

Initial efforts to synthesize calcium-polyP particles performed together with an undergraduate student, Mr. Justin Quan, were based on a published method [71]. In these initial experiments, we investigated the effects of sodium chloride concentration in the buffer, polyP and calcium chloride concentrations, mixing rate, rate of the dropwise addition of the calcium chloride solution into the polyP solution and the pH of the solutions. Some success was achieved in the synthesis of particles with a good polydispersity index (PDI; less than 0.5) and count rate (more than 150 kcps). Some conditions even led to nanoscale particles. However, we came to identify important issues with these early attempts:

(i) An apparent absence of particles stability, as DLS measurements taken after the solution agitation was stopped showed declining count rates and a gel-like substance quickly accumulating at the bottom of sample tubes suggestion settling and agglomeration (Figure 5.1 (A));

(ii) A lack of reproducibility for repeat runs prepared under the same conditions. This was attributed to some degree to particle instability.

(iii) The presence of very large particles (or aggregates), sometimes in the micrometer range, that were also visible by eye (Figure 5.1 (B)).

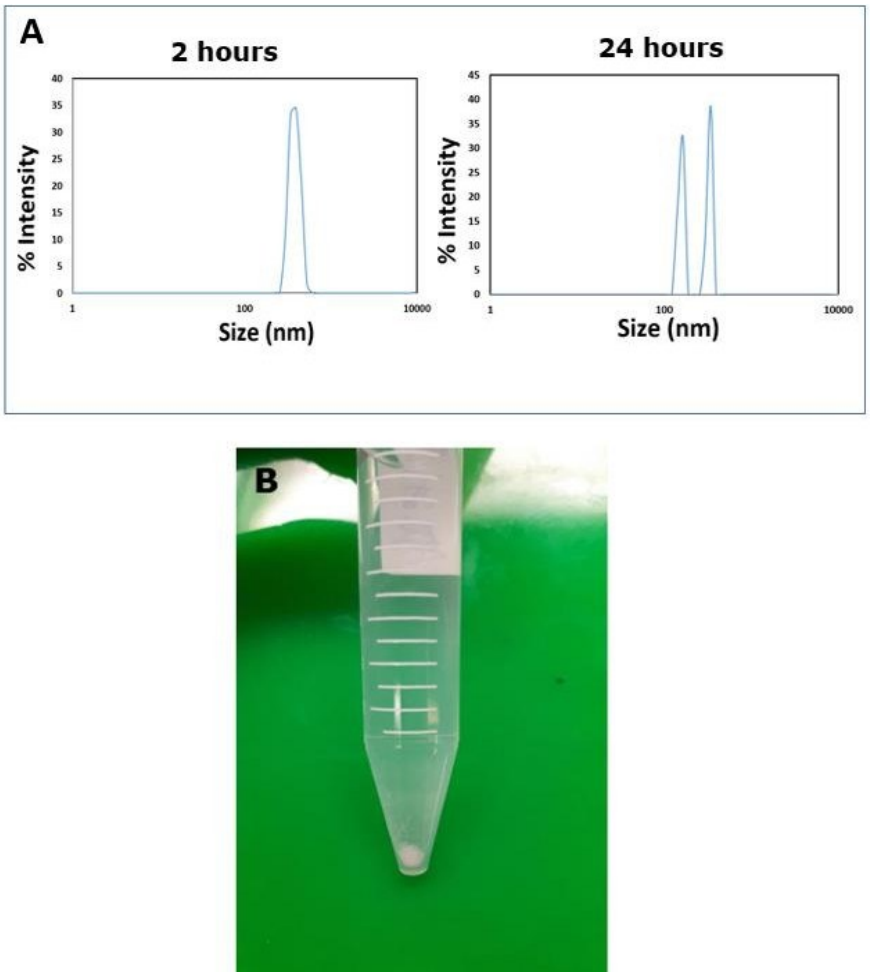

Figure 5.1. (A) Size variation in the particles from 2 hours to 24 hours and (B) Visible particles suggesting the presence of large particles after synthesis.

Through efforts to address these issues, it was discovered that polyP lowers the pH of the buffer solution substantially, such that experiments were performed at a lower pH than intended. This is particularly important for two reasons. Firstly, the rate of polyP hydrolysis increases at

lower pH [53]. Secondly, calcium phosphate precipitation is generally impacted by pH [72]. This was addressed by readjusting the pH of the polyP and calcium chloride solutions prior to the dropwise addition step. Discussions with a collaborator, Dr. Mark Filiaggi from Dalhousie University, lead us to change our approach from adding calcium chloride to the polyP solution to adding polyP to the calcium chloride solution. It was suggested that our initial approach could favor the coacervation rather than precipitation. These changes were not sufficient to fully address the before mentioned issues.

5.2. Citrate-capped calcium-polyP particles

Since data irreproducibility and issues with agglomeration mean that the particles synthesized cannot be considered for further biological studies without complicating the interpretation of results, we wanted to test synthesizing the particles in presence of capping agents. One such compound we considered was sodium citrate dihydrate (SC), which has been used extensively in the synthesis of silver nanoparticles to aid in the stability of the particles after formation. We first synthesized particles according to the protocol described in Chapter 2 (the specific conditions are listed in (Table 5.I) and added an equal volume of 2 mM SC after 1 hour of agitation to make a 1 mM citrate solution. Mixing was continued for an additional 23 hours. This experiment led to the synthesis of sub-micron particles with an average size of 234 nm, which was very close to the Z-average of 264.3±35.02 nm. The size distribution shows a bimodal distribution with particle sizes 230.1±22.84 nm. The PDI was relatively low at 0.37±0.051 suggesting a narrow distribution without and the count rate high at 212.3±34.43 kcps (Figure 5.2).

Table 5.I. Parameters used for synthesizing Ca-polyP particles with Sodium citrate dihydrate

Parameter	Varying range
Mixing rate	500 rpm
NaCl concentration (Ionic strength)	150 mM
pH	10
$CaCl_2$	2 mM
polyphosphate concentration	4 mM
Drop rate	1 mL/min

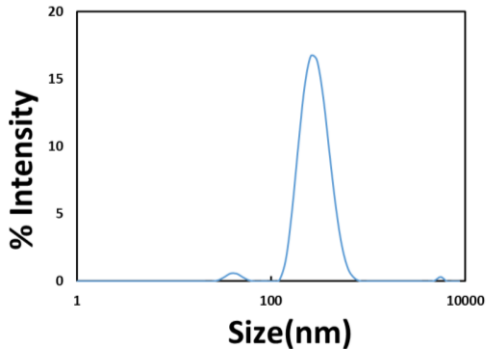

Figure 5.2. Typical size distribution profile measured by DLS for calcium-polyP particles prepared by dropwise addition of polyP into a calcium chloride solution and further addition of sodium citrate after 1 hour of agitation.

5.3. Calcium-polyP particles stability

Given the relatively low PDI observed in particle solutions prepared by adding SC and the apparent absence of large particles/agglomerates, we decided to characterize these particles further. To evaluate their stability over time, samples were incubated at room temperature without agitation and analysed using DLS at different time point up to 96 hours. As can be seen from Figure 5.3., the average size only increased very slightly with time from 303 ± 10.5 nm at day 0 to 313.3 ± 12.7 nm at day 4. Similarly, a slight increase in z-average from 457.8 ± 87 nm at day 0 to 546.5 ± 20.3 nm at day 4 was also observed, while the count rate decreased slightly over time. Taken together, these results were interpreted as suggesting a degree agglomeration

over time, albeit substantially decreased compared to the previous protocol used. It is hypothesized that citrate groups bind to the surface of particles, thereby modifying surface chemistry and the interactions between particles. Future work will require evaluating the surface charges of the particles produced with and without SC to provide some understanding of the mechanism behind this increased stability.

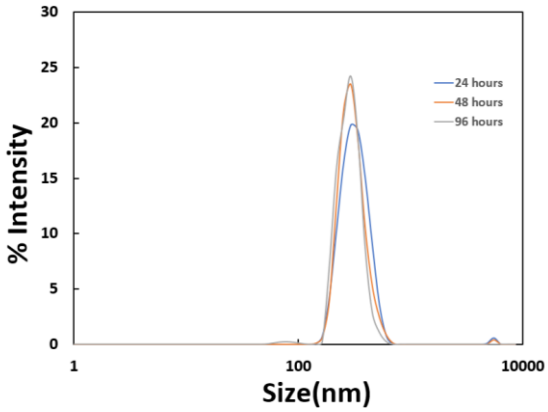

Figure 5.3. Average size variation of the particles with time and without sodium citrate.

5.4. Effect of calcium and polyP concentrations

Next, we sought to identify parameters that can provide a degree of control over average particle size. We first investigated the effects of both calcium and polyP concentrations in the initial solution on the synthesis of particles. To do so, we designed a 3^2 full factorial design experiment with triplicates for each condition. During preliminary stages of particle synthesis, we arrived at the conclusion of obtaining particles of reproducible size by maintaining out drop rate at 1 mL/min, mixing rate at 500 rpm and pH of 10 and therefore maintained these parameters constant in this study.

The solution compositions and results are shown in Table 5.II. and Figure 5.4. The color codes incorporated in the Table indicates combinations of concentrations with similar patterns of results. Conditions marked in green were characterized by PDI less than 0.4, similar average sizes and z-averages and count rates more than 200 kcps. These are considered combinations of

concentrations that provide a sufficient “concentration” of small (i.e. close to nanoscale) and uniform particles. No considerable effect of polyP and calcium concentration on average size was noted for these conditions. Conditions marked in yellow had very low count rates compared to those marked in green. Conditions marked in red had large PDI of more than 0.6, substantial differences between sizes and z-averages, and low count rates less. These results effectively provide limits in the concentrations of polyP and calcium that should be used for particle synthesis.

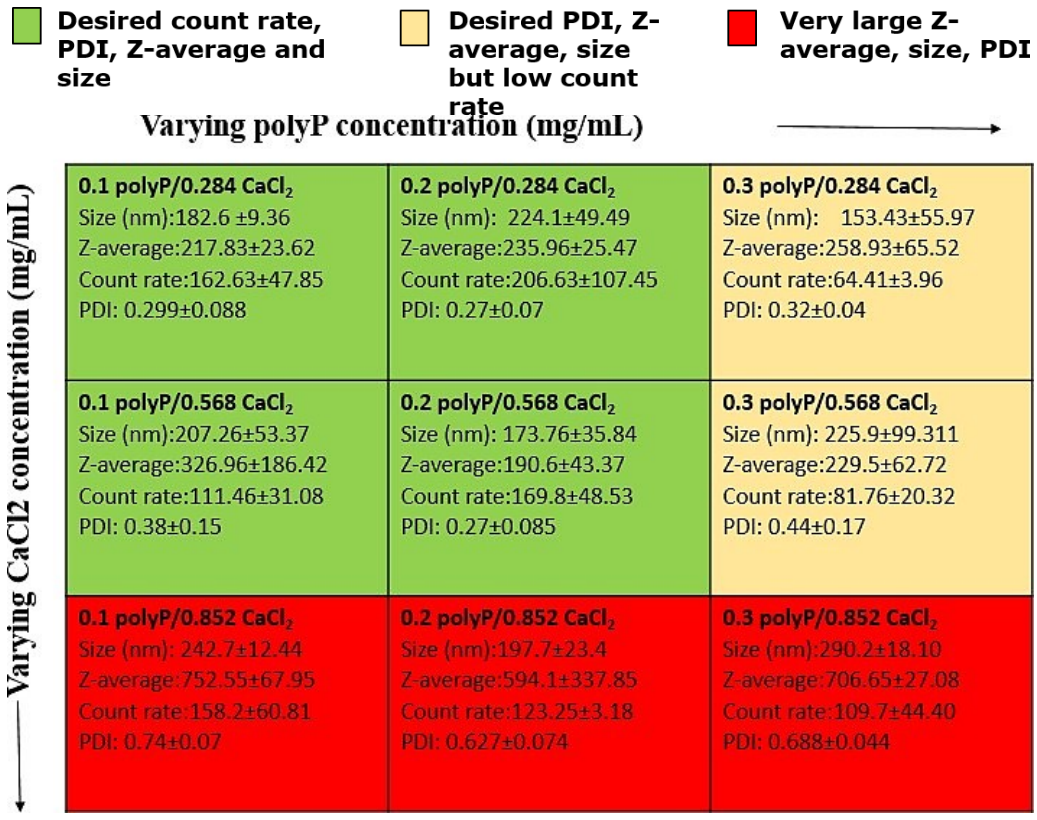

Table 5.I. (A) 3^2 full factorial design experiment to investigate the effects of calcium and polyP concentrations on particle synthesis (B) Average values of size, Z-average, PDI and count rates of the experiment.

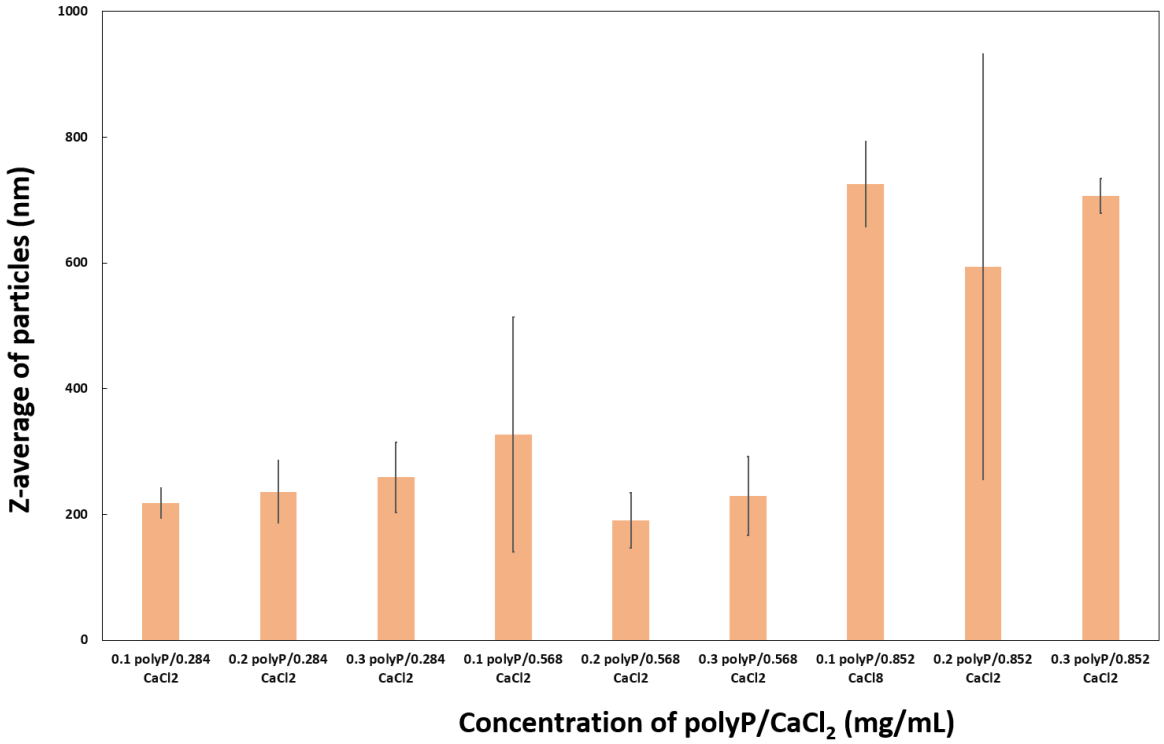

Figure 5.4. Average size variation of the particles with different concentrations of $CaCl_2$ and polyP.

5.5. Effect of pH on calcium-polyP particle synthesis

We also investigated the effect of pH on the formation of particles because a broad range of pH have been reported in the literature for the formation of calcium-polyP particles. Here we investigated pH of 5.5, 7.0 and 8.5 (compared to the previous experiments, which were performed at pH 10.0). We were interested in seeing if this parameter could impact average particle sizes. Both pH 5.5 and 8.5 lead to particle populations with large PDI, important differences between the size and z-average and very low count rates of less than 60 kcps (not much higher than that measured for the buffer alone) as shown in Figure 5.5. Unexpectedly, pH 7.0 lead to particle populations with better PDI and count rates, as well as close average size and z-average values, albeit with an average size larger than that observed at pH 10.0. These results suggest that more agglomeration occurs at lower pH.

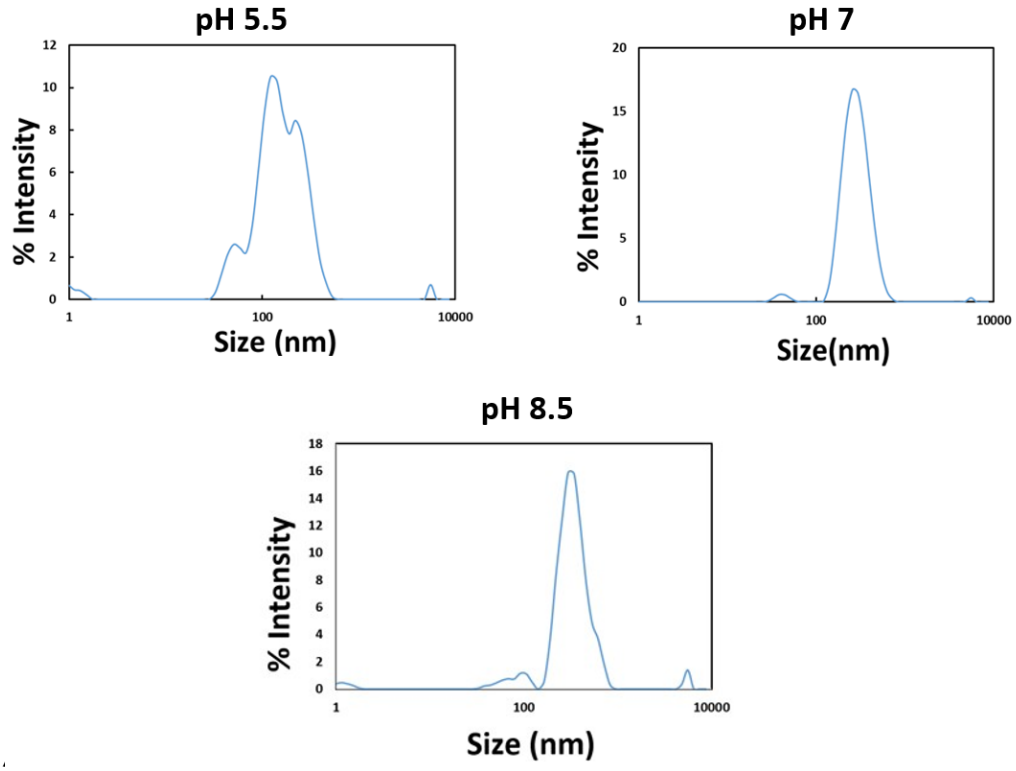

Figure 5.5. Size distribution profiles measured by DLS for calcium-polyP particles prepared by dropwise addition of polyP into a calcium chloride solution at different pH.

5.6. Effect of the timing of SC addition on calcium-polyP particle synthesis

Finally, we wanted to investigate the impact of the timing of our SC addition step on particle size. We chose to maintain the final SC concentration constant but introduced different proportions of the total SC added at the start of the synthesis. Sodium citrate was also added after 1 hour of mixing to ensure to bring up the final concentration to the target of 1 mM. Initial trials had been performed with 0 mM SC at the start and the addition of a volume equal to the synthesis volume of 2 mM SC after mixing had been completed for 1 hour. Here, we added SC concentrations of 0.2, 0.5, and 1 mM at the start of the experiment followed by additions of solutions at 1.8, 1.5, and 1 mM SC after 1 hour of mixing. The best result based on particle size, z-average, count rate and, PDI was obtained for particles prepared by adding 0.5 mM SC prior to

mixing of the precursor solutions and 1.5 mM SC after 1 hour of mixing (Figure 5.6.). This condition produced an average size of 229.4 ± 24.2 nm, while the PDI was 0.485 ± 0.1, with a z-average of 256±12.5 and count rate of 160.4±9.8 kcps.

SEM imaging of the particles produced with these conditions is shown in Figure 5.7. SEM showed that the particles produce with the optimized procedure are generally spherical with what appears to be a broader size distribution than was reported by DLS. It is uncertain at this point if this is a consequence of the areas on the sample that were imaged or if the procedure to prepare the samples for imaging led to the agglomeration of smaller particles.

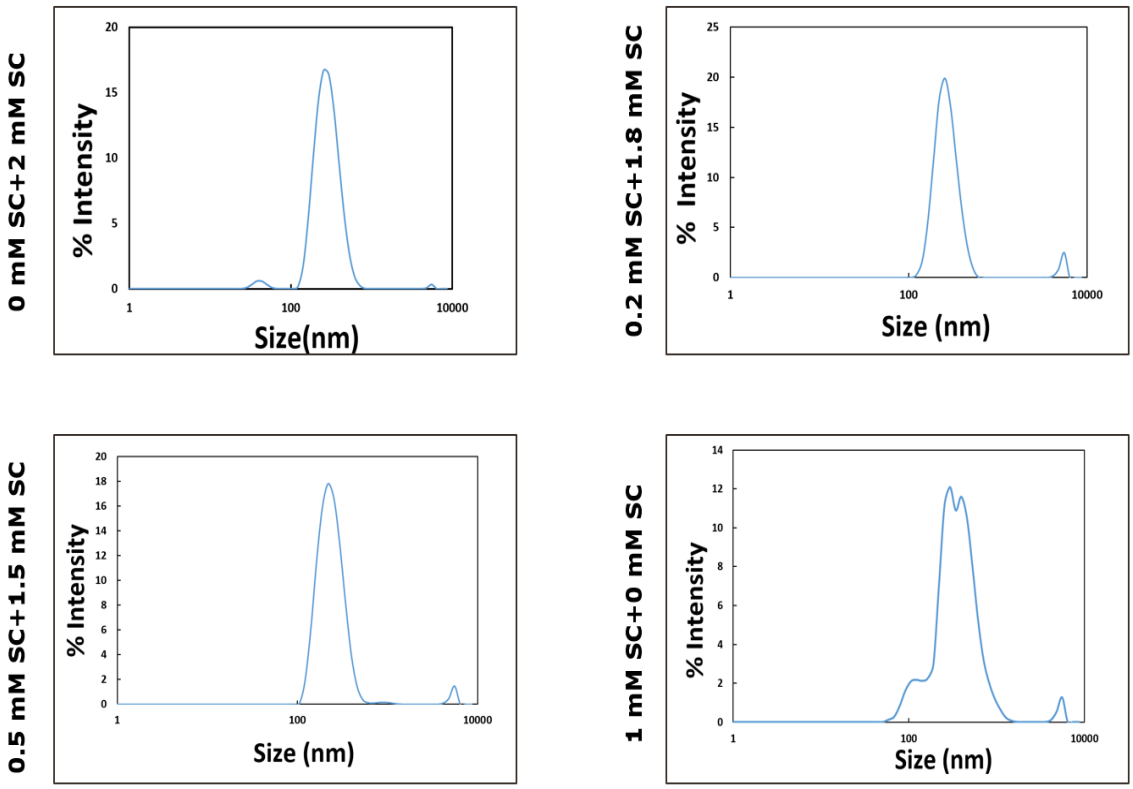

Figure 5.6. Size distribution profiles measured by DLS for calcium-polyP particles prepared by dropwise addition of polyP into a calcium chloride solution with different citrate addition protocols.

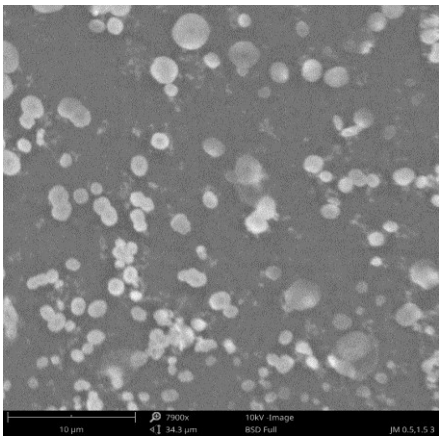

Figure 5.7. SEM image of sub-micron calcium-polyP particles showing a relatively broad distribution of spherical particles.

5.7. Sterilization and dispersion of calcium-polyP particles in cell culture medium

We also evaluated a number of strategies to isolate the particles from the synthesis solution, allow the measurement of particle concentrations, sterilize them for cell culture experiments and resuspend them in cell culture medium. SC-capped calcium-polyP particles were dialysed, lyophilized, and sterilized in 70% ethanol, before being dispersed in culture medium (DMEM with 10% FBS and 1% antibiotics). DLS measurements indicated a size of 550 nm and z-average of 600 nm with count rate of 100 kcps and PDI of 0.999 at the end of this procedure (Figure 5.8.). A control was also performed whereby just the supplemented DMEM (i.e. without particles) was analyzed with DLS (Figure 5.8.A). This control showed peaks at small sizes that reflect similar peaks in the sample containing particles. These peaks were attributed to protein agglomeration and do not reflect the size of particles. The remaining peaks in the sample containing particles are much larger than in the samples prior to processing. These results suggest that the process may have led to particle agglomeration. While more studies are required to determine if this agglomeration is the result of proteins in the solution, modifications will likely need to be made in the protocol to ensure that the particles do not agglomerate and can

penetrate AC if injected into a joint capsule.

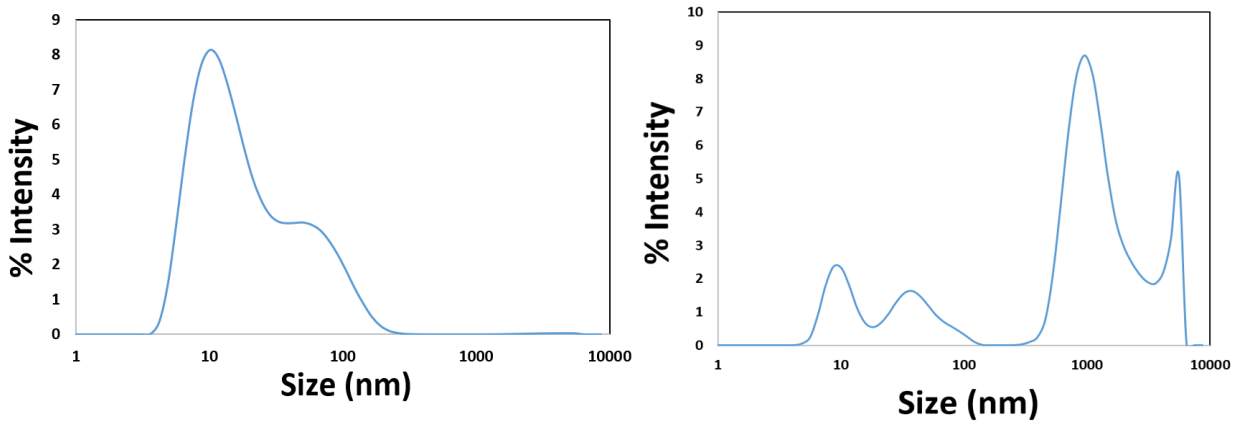

Figure 5.8. Size variation in the DMEM with 10% FBS and 1% antibiotics (left) and in the DMEM with 10% FBS and 1% antibiotics and the particles synthesized with 0.5 mM Sodium citrate in the buffer before synthesis.

5.8. Summary

In the second part of this project, we developed a protocol for synthesizing calcium-polyP nanoparticles with the addition of SC that aids in reducing the degree of agglomeration of the particles. This protocol can be used for producing sub-micron particles; however, we have yet to achieve the synthesis of nanoparticles, which will be a future objective of this project. We also have studied the effects of polyP and calcium concentrations, as well as pH and concentration of SC on the particle size and found minimal effects within the ranges investigates. Agitation conditions and sodium chloride concentration will be re-evaluated with this modified protocol incorporating SC. Our early results have shown an impact of these parameters on size and the concentration of sodium chloride was found by others to have an important effect on polyP size [95].

Particles must be resuspended into appropriate culture media for further biological characterization and would eventually need to be injected within the synovial fluid in the joint in order to be used as a therapeutic. In this study, we have observed agglomeration in our initial

efforts to achieve this goal. This will need to be addressed in the next phase of the project.

CHAPTER 6 – CONCLUSIONS, LIMITATIONS AND FUTURE WORK

6.1. Conclusions

In this thesis, we were first able to establish that polyP does elicit FLS cell responses. Indeed, it was shown that the bioactive inorganic polymer inhibits FLS cell proliferation. This is an interesting effect because FLS cell proliferation has been associated with the development of OA. Treatment of FLS cells with polyP also led to changes in the metabolic activity and the migration rate of FLS, although it remains unclear how these data fit within the context of the use of polyP as an OA therapeutic. We also developed a new protocol to synthesize sub-micron citrate-stabilized calcium-polyP particles. These particles were shown in cell culture to be non-cytotoxic at concentrations for which they are bioactive by Mr. Justin Quan (data not discussed in the thesis). This thesis represents a first step towards the ultimate goal of developing targeted and sustained delivery vehicles for the prolonged release of polyP in the joint following intra-articular injection. Such a technology would represent a powerful approach for the treatment of early stage OA.

6.2. Limitations

Over the course of the thesis, a number of issues have limited the progression of the work. In regard to our first objective, which aimed to characterize the responses of FLS to the exogenous administration of polyp, the main limitation faced stemmed from our inability to elicit an effect on the FLS cells with the administration of IL1β. This cytokine is often used in the field to model the effects of inflammation on FLS cells. The successful implementation of this model would have allowed us to study the effects of polyP on the inflammatory-responses of FLS cells, making the data much more relevant to the ultimate therapeutic goal of the research. In regard to

our second objective, we identified two key limitations of our strategy that have slowed the progression of the work substantially. We have found that it was difficult to produce particles with (1) reproducible and (2) stable sizes. These issues need to be addressed prior to investing time into understanding the parameters that allow a degree of control over particle size.

6.3. Future work

While this thesis led to progress on two fronts of the broader project, there remains substantial amount of work to be done towards the use of polyP as a therapeutic molecule for OA treatment.

6.2.1. Objective 1

As pertains to our first objective, it will be important to:

1. Establish a cytokine treatment that elicits an inflammatory response in bovine FLS cells as a mandatory first step to the continuation of the project.
2. Determine the effects of polyP on FLS phenotypic changes associated with an inflammatory response.
3. Investigate the bioenergetic effects of polyP on cells in the joint including FLS cells.

As a long-term objective, it will be essential to determine the mechanism of action and signaling pathways involved in the response of FLS cells (and chondrocytes) to polyP. The effects of polyp on these cell types are only beginning to be elucidated and the use of any bioactive molecules as therapeutics for the treatment of diseases requires an in depth understanding of the molecular mechanisms involved with the biological effects.

6.2.2. Objective 2

With regards to the synthesis of calcium-polyP particles, we have established a proof-of-concept protocol; however, towards facilitating the entry of these particles inside tissues and increasing their retention, the main steps will be to:

1. Optimize synthesis parameters to achieve nanoscale particles that will facilitate entry into AC.
2. Characterize the zeta-potential of particles before and after the addition of citrate to gain insight on surface charge and stability of the colloidal dispersion.

In the long-term, this project would require the development of functionalization strategies (e.g., with short peptides) to increase/control the retention and/or cell internalization of the particles.

REFERENCES

[1] Alice J. SophiaFox, Aheesh Bedi and Scott A.Redeo, "The basic sience of articular cartilage;Structure,composition and function," Sports medicine and shoulder service, , pp. 461-468, 2009.

[2] B.Richardson, Abhijit M.Bhosle and James, "Articular cartilage:Structure,injuries and review of management," British medical Bulletin, vol. 87, pp. 77-95, 2008.

[3] Rebekah S.Decker, Eiki Koyama,Maurizio Pacifici, "Articular cartilage:structural and developmentall intricacies and questions," HHS Public access, vol. 13(6), pp. 405-414, 2015.

[4] Hooi Yee Mg, Kai-Xing Alvin Lee and Yu-Fang shen, "Articular cartilage: Structure, Composition, Injuries and Repair," SciMed Central, vol. 1(2), no. 1010, pp. 1-6, 2017.

[5] Carl Orr, Elsa Sousa, David L.Boyle, Maye H.Buch, christoper D.Buckley, "Synovial tissue research: a state-of-art review," Nature reviews Rheumatology 13, pp. 462-475, 2017.

[6] JP St-Pierre, Qishan Wang,Shu Qiu Li,Robert M.Pilliar and Rita A.Kandel., "Inorganic polyphosphate stimulates tissue formation," Tissue Engineering, vol. 18, , pp. 1282-1292, 2012.

[7] Georgina E. Lang, Peter S. Stewart, Dominic Vella, Sarah L. Waters,and Alain Goriely," Is the Donnan effect sufficient to explain swelling in brain tissue slices?", J R Soc Interface. 2014 Jul 6; 11(96): 20140123., vol. 11(96), 2014.

[8] Nohe, Hemanth Akkiraju and Anja, "Role of chondrocytes in cartilage formation,progression of Osteoarthritis and cartilage regeneration," HHC Public access, vol. 3(4), , pp. 177-192, 2015.

[9] A.Robert Poole, Tadashi Asuda, Asahiko Obayasha, "Composition and structure of Articular cartilage-A template for tissue repair," in Cartilage Biology, Clinical Orthopaedics and related research, 2001, pp. S26-S32.

[10] Joseph Withrow, Cameron Murphy, Yutao Liu, Monte Hunter, Sanddanand Fulzele and Mark W. Hamrick., "Extracellular vesicles in the pathogenesis of rheumatoind arthritis an dosteoarthritis," Arthritis research and therapy, vol. 18:286,2016.

[11] Neal X Chen, kalisha D O'Neil, Xianming Chen and Sharon M Moe"Annexin-mediated matrix vesicle Calcification in vascular smooth muscle cells," Journal of bone and mineral research, vol. 23, 2008.

[12] Hashimoto S, Ochs RL, KomiyaS, Lotz M"Linkage of chondrocyte apoptosis and cartilage degradation in human osteoarthritis," Arthritis Rheum, vol. 41(9), no. 1592-8, 1998.

[13] H.Clarke Anderson, MD Cureent, "Matrix vesicles and calcification," Rhematology reports, vol. 5, pp. 222-226, 2003.

[14] G. EE, "Role of matrix vesicles in biomineralization," Biochem biophys Acta., vol. 2, p. 1790, 2009.

[15] Jos Malda, Janeke Boere, Chris H.A. van de lest, "Extracellular vesicles-new tool to repair and regeneration," Natural reviews rheumatology, vol. 5, pp. 243-249, 2016.

[16] V. J. Langer R, Tissue Engineering science, vol. 510, no. 920-6, p. 260, 1993.

[17] Mads S Bergholt, Jean-Philippe St-Pierre,Giovanni S Offendu, Paresh A Parmer,Micheal B Albro,Jenniefer L Puetzer,Molly M Stevens., "Raman Spectroscopy rveals new insights into the zonal organaization of tissue engineered articular cartilage," American chemical society, vol. 2, no. 12, pp. 885-895, 2016.

[18] Shapiro F, Koide S, Glimcher MJ. Cell origin and differentiation in the repair of full-thickness defects of articular cartilage. J Bone Joint Surg Am,75(4):532-53,1993.

[19] C. E. Anderson, "Formation, Structure and function of cartilage," California medicine, vol. 91, no. 6, pp. 321-326, 1959.

[20] Massimo bottani, Kunal Bhattacharya,Bengt Fadeel,Andrea Magrini,Nunzio Bottini,Nicola Rosata, "Nanodrugs to target articular cartilage: An emerging platform for osteoarthritis therapy," Elsevier, vol. 12, pp. 255-268, 2016.

[21] Katie M. Yocham ,Crystal Scott ,Kiyo Fujimoto ,Raquel Brown ,Emily Tanasse ,Julia T. Oxford ,Trevor J. Lujan ,David Estrada, Mechanical Properties of Graphene Foam and Graphene Foam—Tissue Composites Volume 20, Issue 9 ,2018

[22] Huading Lu ,Yuhu Dai ,Lulu Lv, Huiqing Zhao, Chitosan-Graft-Polyethyleneimine/DNA Nanoparticles as Novel Non-Viral Gene Delivery Vectors Targeting Osteoarthritis January 2, 2014.

[23] Matthias jacobi, Vincent Villa,Robert A Magnussen and Philippe Nyret, "Sports Med," Arthose Rehabil Ther Technol, vol. 3:10, 2011.

[24] E.B.Hunziker, K Lippuner,M.J.B. Keel,N.Shintani, "Osteoarthritis and cartilage-An educational review of cartilage repair;precepts and practise-myth and misconceptions-progress and prospects," Osteoarthritis research society, vol. 12, pp. 1063-4584, 2014.

[25] Venkatesh Ponemone, Saniya Gupta,Manish Suthar, "Energing Potential of cell based therapies for articular cartilage repair and regeneration," Semantic scholar, no. 2017.

[26] Janani mahendran,JP St-Pierre, Nanomaterials Applications in Cartilage tissue engineering, Springer Nature, 1-27,2019.

[27] Jorge L.Escobar Ivirico, Maumita Bhattacharjee, Emmanuel Kuyinu, Lakshmi S.Nair Regenerative Engineering for Knee Osteoarthritis Treatment: Biomaterials and Cell-Based Technologies volume 3, Issue 1, pp 16-27,2017.

[28] Hellio le Graverand MP, Clemmer RS,Redifer P,Brunell RM,Hayes CW,Brandt KD,Abramson SB,Manning PT,Miller CG,Vignon E., "A 2-year randomised ,double-

blind,placebo-controlled,multicnter study of oral selective iNOS inhibitor,cindunistat(SD-6010) in patients with symptomatic Osteoarthritis of the knee.," Annals of teh Rheumatic diseases, vol. 72(2), pp. 187-95, 2013.

[29] Pavelka K, Bruyere O,Cooper C,Kanis JA,Leeb BF,Maheu E,Martel-PelletierJ,MontfortJ,Pelletier JP,Rizzoli R,Reginster JY, "Diacerin benefits,Risks and palce in management of Osteoarthritis An Opinion-based report from ESCEO," Drugs and Aging, vol. 33(2), pp. 75-85, 2016.

[30] Karsdal MA, Byrjalsen I,Alexanderson P,Bihlet A,Anderson JR,Riis BJ,Bay-Jensen AC,Christiansen C, "Treatment of symptomaticknee osteoarthritis with oral salmon calcitonin results from two phase 3 trials," Osteoarthritis and Cartilage, vol. 23(4), pp. 532-43, 2015.

[31] Reginster J, Badurski J,Bellamy N,Bensen W,Chapurlat R, Chevalier X, Christiansen C, Genant H,Navarro F,Nasanov E,Sambrook PN,Spector TD,Cooper C, "Efficacy and safety of strontium ranelate in the treatment of knee osteoarthritis: results of a double-blind, randomised placebo-controlled trial," Annals of the Rheumatic diseases , vol. 72(2), pp. 179-86, 2013.

[32] Lohmander L.S., Hellot S., Dreher D., Krantz E.F., Kruger D.S., Guermazi A., Eckstein F., "Intraarticular sprifermin (recombinat human fibroblast growth factor 18) in knee osteoarthritis:a randomized double-blind,placebo-controlled trial," Arthritis and Rheumatology., vol. 66(7), pp. 1820-31, 2014.

[33] Hunter D.J., Pike M.C., Jonas B.L., Kissin E., Krop J., McAlindon T., "Phase 1 safety and tolerability study of BMP-7 in symptomatic knee osteoarthritis," BMC Musculoskelet Disord., vol. 232, p. 11, 2010.

[34] D. Yu S.P.Hunter, "Intra-articular therapies for osteoarthritis," Expert opinion on Pharmacotherapy, vol. 17(15), pp. 2057-71, 2016.

[35] Dietrich Pape, Giuseppe Filardo, Elisaveta Kon, C.Niek van Dijk and Henry Madry., "Disease specific problems associated with the subchondral bone," Springer, no. 10.1007/s00167-010-1052-1, 2009.

[36] M. Brittberg, "Autologous chondrocyte Implantation-Technique and long-term follow-up," Cartilage surgery,pp 40-49, 2011.

[37] M. Banfy, Orthopedic Sports Medicine and Joint Preservation,www.kerlanjobe.org.

[38] Alpaslan Oztürk, corresponding author M. Recai Ozdemir, and Yüksel Ozkan "Osteochondral autografting (mosaicplasty) in grade IV cartilage defects in the knee joint: 2- to 7-year results," vol. 30, no. 3, 2006.

[39] M. F. f. M. E. a. Research, www.mayoclinic.org.

[40] Syed A.A.Rizvi, Ayman M.Saleh, “Applications of nanoparticle systeh in drug delivery technology”, Saudi Pharmaceutical Journal, pp 64-70, 2018.

[41] W.H.Viotto, A.P.Barth and C.F.Tormaena, "Amorphous Ca2+ polyphosphate nanaoparticles repulate the ATP level in bone-like SaOS-2 cells," The compass of Biologists, vol. 128, pp. 2202-2207, 2015.

[42] Lutolf MP, Hubbell JA, "Synthetic biomaterials as instructive extracellular microenvironments for morphogenesis in tissue engineering.," vol. 23, no. 1, pp. 47-55, 2005.

[43] Lutolf MP1, Weber FE, Schmoekel HG, Schense JC, Kohler T, Müller R, Hubbell JA, "Repair of bone defects using synthetic mimetics of collagenous extracellular matrices.," vol. 21, no. 3, pp. 51-8, 2003.

[44] Jayanta Kumar Patra, Gitishree Das, Leonardo Fernandes Fraceto, Estefania Vangelie Ramos Campos, Maria del Pilar Rodriguez-Torres, Laura Susana Acosta-Torres, Luis Armando Diaz-Torres, Renato Grillo, Mallappa Kumara Swamy, Shivesh Sharma, Solomon Habtemar,

"Nano based drug delivery systems: recent developments and future prospects," Journal of nanobio-technology, vol. 16, 2018.

[45] Y. L. a. C. W. Mona Alizadeh-Osgouei, "A comprehensive review of biodegradable synthetic polymer-ceramic composites and their manufacture for biomedical applications," Bioactive Materials, vol. 4, no. 1, pp. 22-36, 2018.

[46] S. H. Tao et al. "Therapeutic potential of hyaluronic acid/chitosan nanoparticles for the delivery of curcuminoid in knee osteoarthritis and an in vitro evaluation in chondrocytes," International journal of molecular medicine, pp. 2604-2614, 2018.

[47] Asmaa S. El-Houssiny et al. " Volume 9, Issue 3-4," European Journal of Nanomaedicine, vol. 9, no. 3-4, 2017.

[48] Xiuling et al."Glucosamine sulphate-loaded distearoyl phosphocholine liposomes for osteoarthritis treatment: combination of sustained drug release and improved lubrication," Bimoaterials Science, no. 7, 2019.

[49] A. Kornberg, "Inorganic polyphosphate:Toward making a forgotten polymer unforegttable," Journal of Bacteriology, vol. 177, pp. 491-96, 1995.

[50] Prabhakar Tiwari, Tannu Priya Gosain, Mamta Singh, "Inorganic polyphosphate accumulation suppresses the dormancy response and virulence," JBC Papers in Press, pp. 2-17, 2019.

[51] Alexander J.Donovan, Joseph Kalkowski, Stephanie A.Smith,James H.Morrissey and Yiung Liu, "Size-controlled synthesis of granular polyphosphate nanoparticles st physiologic salt concentrations for blood clotting," Biomacromolecules, vol. 15, pp. 3976-3984, 2014.

[52] Müller WE, Tolba E, Schröder HC, Diehl-Seifert B, Wang X. “Retinol encapsulated into amorphous Ca(2+) polyphosphate nanospheres acts synergistically in MC3T3-E1 cells”, volume 93, 213-244, 2015.

[53] C. A.P.Barth, "pH influences hydrolysis of sodium polyphosphate in dairy matrices and the structure of processed cheese," Journal of dairy Science, vol. 100, no. 11, pp. 8735-8743, 2017.

[54] K.Lortz, Shigeru Miyaki and martin, "Extracellular vesiclesin cartilage homeostasis and Osteoarthritis," Curr Opin Rheumatol, vol. 30, pp. 129-135, 2018.

[55] "Efficacy and safety of strontium ranelate in the treatment of knee osteoarthritis: results of a double-blind, randomised placebo-controlled trial". Ann Rheum Dis,2013.

[56] M. Banffey, Orthopedic Sports Medicine and Joint Preservation.

[57] Neus G Bastus, "Synthesis of Highly monodisperse citrate-stabilized silver nanoparticles of up to 200 nm:Kinetic control and catalytic properties," Chemistry o fmaterials, vol. 26, pp. 2836-2846, 2014.

[58] Portero A, Remunan-Lopez C, Criado M, Alonso M, "Reacetylated chitosan microspheres for controlled delivery of anti-microbial agents to the gastric mucosa," J Microencapsul. , pp. 797-809, 2002.

[59] Artursson P, Lindmark T, Davis SS, Illum L, "Effect of chitosan on the permeability of monolayers of intestinal epithelial cells (Caco-2).," Pharm Res. , vol. 11, pp. 1358-1361, 1994.

[60] Fernández-Urrusuno R, Calvo P, Remuñán-López C, Vila-Jato JL, Alonso MJ., "Enhancem," Pharm Res., vol. 16, pp. 1576-81, 1996.

[61] De Campos AM, Sánchez A, Alonso MJ, "Chitosan nanoparticles: a new vehicle for the improvement of the delivery of drugs to the ocular surface. Application to cyclosporin A.," Int J

Pharm., pp. 159-68, 2001.

[62] Al-Qadi S, Grenha A, Carrión-Recio D, Seijo B, Remuñán-López C, "Microencapsulated chitosan nanoparticles for pulmonary protein delivery: in vivo evaluation of insulin-loaded formulations.," J Control Release, vol. 157, pp. 383-90, 2012.

[63] Liu S, Yang S, Ho PC, "Intranasal administration of carbamazepine-loaded carboxymethyl chitosan nanoparticles for drug delivery to the brain.," Asian J Pharm Sci. , vol. 13, pp. 72-81, 2018.

[64] S. A., "Alginate particles as platform for drug delivery by the oral route: state-of-the-art.," ISRN Pharm, no. 2014:926157, 2014.

[65] W. S. Gombotz WR, "Protein release from alginate matrices.," Adv Drug Deliv Rev. , pp. 267-85, 1998.

[66] Haque S, Md S, Sahni JK, Ali J, Baboota, " Development and evaluation of brain targeted intranasal alginate nanoparticles for treatment of depression," J Psychiatr Res., vol. 48, pp. 1-12, 2014.

[67] Garrait G, Beyssac E, Subirade M, "Development of a novel drug delivery system: chitosan nanoparticles entrapped in alginate microparticles.," J Microencapsul., vol. 31, pp. 363-72, 2014.

[68] Kulthe SS, Choudhari YM, Inamdar NN, Mourya V, "olymeric micelles: authoritative aspects for drug delivery.," Design Monomers Polym. , vol. 15, pp. 465-521, 2012.

[69] Choi S-J, Lee JK, Jeong J, Choy J-H., "Toxicity evaluation of inorganic nanoparticles: considerations and challenges.," Mol Cell Toxicol. , vol. 9, pp. 205-10, 2013.

[70] M. A. Bozzuto G, "Liposomes as nanomedical devices.," Int J Nanomed. , vol. 10, p. 975, 2015.

[71] Werner E.G.Muller, Emad Tolba, Shunfeng Wang, "A new polyphosphate calcium material with morphogenetic activity", Elsevier., vol148, pp.163-166,2015.

[72] Niemeyer R. “Cyclic condensed metaphosphates and linear polyphosphates in brown and red algae”. Arch Microbiol 108(3):243-7,1976.

[73] Kulaev IS, Vagabov VM, Kulakovskaya TV. “The Biochemistry of Inorganic Polyphosphates”. Chichester, England: John Wiley & Sons, Ltd; 2004.

[74] Terkeltaub RA. “Inorganic pyrophosphate generation and disposition in pathophysiology”. Am J Physiol Cell Physiol 281(1):C1-C11, 2011.

[75] Wiame JM. Yeast metaphosphate. Fed Proc 6(1):302,1947.

[76] Lucia A,Jozef N.”Polyphosphate-an ancient energy source and active metabolic regulator”,2011.

[77] Yan Wang,Min Lin,Pei Li,Haijun Teng, Dehong Fan.”Progress and Applications of Polyphosphate in Bone and Cartilage regeneration”, 5141204(12), 2019.

[78] Kumble KD, Kornberg A. “Inorganic polyphosphate in mammalian cells and tissues”. J Biol Chem 270(11):5818-22, 1995.

[79] Lihan Xie,Ursula Jakob . “Inorganic polyphosphate, a multifunctional polyanionic protein scaffold”, 10.1074-20,2018.

[80] Pisoni RL, Lindley ER. “Incorporation of [32P]orthophosphate into long chains of inorganic polyphosphate within lysosomes of human fibroblasts”. J Biol Chem 267(6):3626-31,1992.

[81] Justin Lempart, Ursula Jakob. “Role of Inorganic polyphosphate in Amyloidogenic processes Cold Spring Harbor Perspectives in Biology”;201:e00070-19,2019.

[82] Qingyan Lin, Heqing Huang, Liying Chen and Guixiu Shi, "Synthesis of caffeic acid coated silver nanoparticles for the treatment of osteoarthritis" ,Volume 28, Issue 3, 2017.

[83] Syed A.A.Rizvi, Ayman M.Saleh, Applications of nanoparticle system in drug delievry technology", Saudi Pharmaceutical Journal, 64-70, 2018.

[84] Blanco FJ,et al., "Osteoarthritis chondrocytes die by apoptosis.A possible pathway for osteoarthritis pathology",Arthritis Rheum,1998.

[85] Zhou P. Qiu B. Deng R. Li H. Xu X. Shang X.,"Chondroprotective Effects of Hyaluronic Acid-Chitosan Nanoparticles Containing Plasmid DNA Encoding Cytokine Response Modifier A in a Rat Knee Osteoarthritis Model", 1207-1216, 2018.

[86] Md. Meraj Ansari,Rakesh Kumar Mishra,Syed Shadab Raza Rehan Khan, "Zinc Gluconate-Loaded Chitosan Nanoparticles Reduce Severity of Collagen-Induced Arthritis" in Wistar Rats, 5,7,2019.

[87] Xiaoling Zhang,Changlong Yu,Xushi,Kerong Dai, "Direct chitosan-mediated gene delivery to the rabbit knee joints", 341(1):201-2018,2006.

[88] Shohreh Fattahpour ,Morteza Shamanian ,Naser Tavakoli ,Mohammadhossein Fathi Saeid Reza Sheykhi ,Shirin Fattahpour, "Design and optimization of alginate−chitosan−pluronic nanoparticles as a novel meloxicam drug delivery system", 2015.

[89] S.Daisy Chella Kumari , C.B.Tharani , N.Narayanan , C.Senthil Kumar, "Formulation and characterization of Methotrexate loaded sodium alginate chitosan Nanoparticles", 2013.

[90] Shardool Jain, Thanh-Huyen Tran, and Mansoor Amiji, "Macrophage Repolarization with Targeted Alginate Nanoparticles Containing IL-10 Plasmid DNA for the Treatment of Experimental Arthritis", 162-177, 61, 2016.

[91] Arjmandi M, Ramezani M,"Mechanical and tribological assessment of silica nanoparticle

alginatepolyacrylamide nanocomposite hydrogels as a cartilage replacement".Journal of the Mechanical Behavior of Biomedical Materials. 95:196-204.,2019.

[92] Rakeshchandra R Meka,Shivaprasad H Venkatesha,Bodhraj Acharya & Kamal D Moudgil, "Peptide-targeted liposomal delivery of dexamethasone for arthritis therapy", 14(11), 2019.

[93] Virgínia M Gouveia, José Lopes-de-Araújo,Sofia A Costa Lima, Cláudia Nunes & Salette Reis, "Hyaluronic acid-conjugated pH-sensitive liposomes for targeted delivery of prednisolone on rheumatoid arthritis therapy", Vol 13, No 9, 2018.

[94] A.A. Thorpe1 , S. Creasey2 , C. Sammon2 and C.L. Le Maitre1, "hydroxyapatite nanoparticle injectable hydrogel scaffold to support osteogenic differentiation of human mesenchymal stem cells" , 1-23;vol 32, 2016.

[95] Lorenz B, Leuck J, Kohl D, Muller WE, Schroder HC. "Anti-HIV-1 activity of inorganic polyphosphates. J Acquir Immune Defic Syndr Hum Retrovirol" ,14(2):110-8,1997.

[96] Emanuele Mauri,1 Anna Negri,1 Erica Rebellato,1 Maurizio Masi,1 Giuseppe Perale,2 and Filippo Rossi1, "Hydrogel-Nanoparticles Composite System for Controlled Drug Delivery", 4(3), 2018.

[97] Rajveer Kaur1 , Vishal Kumar Gupta2 and Suresh Chandra Pandey2 ,"Preparation and Evaluation of Hydrogel Nanoparticles as Drug Delivery System", Journal of J Nanomedicine & Nanotechnology,10:1, 2019.

[98] Berrin KÜÇÜKTÜRKMEN, Umut Can ÖZ, Asuman BOZKIR, "In Situ Hydrogel Formulation for Intra-Articular Application of Diclofenac Sodium-Loaded Polymeric Nanoparticles", 56-64, 14(1), 2016.

[99] Xiaohong Wang, Heinz C. Schröder and Werner E. G. Müller, "Amorphous polyphosphate, a smart bioinspired nano-/bio-material for bone and cartilage regeneration:

towards a new paradigm in tissue engineering", 2018.

[100] Werner E. G. Müller ,Shunfeng Wang ,Emad Tolba ,Meik Neufurth ,Maximilian Ackermann ,Rafael Muñoz- Espí ,Ingo Lieberwirth ,Gunnar Glasser ,Heinz C. Schröder ,Xiaohong Wang, "Transformation of Amorphous Polyphosphate Nanoparticles into Coacervate Complexes: An Approach for the Encapsulation of Mesenchymal Stem Cells",2018.

[101] Gabriella M. Fernandes-Cunha, Colin J. McKinlay, Jessica R. Vargas, Henning J. Jessen, Robert M. Waymouthand Paul A. Wender,"Delivery of Inorganic Polyphosphate into Cells Using Amphipathic Oligocarbonate Transporters", 4(10),1394-1402,2011.

[102] Lutolf MP, Weber FE, Schmoekel HG, Schense JC, Kohler T, Müller R, Hubbell JA, "Repair of bone defects using synthetic mimetics of collagenous extracellular matrices.," vol. 21, no. 3, pp. 51-8, 2003.

Appendix 1- List of Permissions for the images used in the thesis

Figure 2.1-Articular cartilage location in a knee joint

This Agreement between Janani Mahendran ("You") and Springer Nature ("Springer Nature") consists of your license details and the terms and conditions provided by Springer Nature and Copyright Clearance Center.

License Number	4727781107660
License date	Dec 14, 2019
Licensed Content Publisher	Springer Nature
Licensed Content Publication	Journal of Bio- and Tribo-Corrosion
Licensed Content Title	Advances in Bio-inspired Tribology for Engineering Applications
Licensed Content Author	Arpith Siddaiah, Pradeep L. Menezes
Licensed Content Date	Jan 1, 2016

Figure 2.2-Zonal arrangement of AC

This Agreement between Janani Mahendran ("You") and Springer Nature ("Springer Nature") consists of your license details and the terms and conditions provided by Springer

Nature and Copyright Clearance Center.

License Number	4727780805303
License date	Dec 14, 2019
Licensed Content Publisher	Springer Nature
Licensed Content Publication	Springer eBook
Licensed Content Title	Nanomaterials Applications in Cartilage Tissue Engineering
Licensed Content Author	Janani Mahendran, Jean-Philippe St-Pierre
Licensed Content Date	Jan 1, 2019

Figure 2.3-Structural differences between a normal ,healthy knee and knee affected with OA

Obtained from the Open access article, "Emerging potential of cell based therapies for articular cartilage repair and regeneration", by Venkatesh Ponemone, Saniya Gupta and Manish Suthar [25] in Advances in Tissue engineering and regenerative medicine.

Figure 2.4-Schematic diagram of marrow stimulation process

This Agreement between Janani Mahendran ("You") and Springer Nature ("Springer Nature") consists of your license details and the terms and conditions provided by Springer Nature and Copyright Clearance Center.

License Number	4655070698186
License date	Aug 23, 2019

Licensed Content Publisher	Springer Nature
Licensed Content Publication	Knee Surgery, Sports Traumatology, Arthroscopy
Licensed Content Title	Disease-specific clinical problems associated with the subchondral bone
Licensed Content Author	Dietrich Pape, Giuseppe Filardo, Elisaveta Kon et al
Licensed Content Date	Jan 1, 2010

Figure 2.5-Illustration of Autologous chondrocyte Implantation

This Agreement between Janani Mahendran ("You") and Elsevier ("Elsevier") consists of your license details and the terms and conditions provided by Elsevier and Copyright Clearance Center.

License Number	4655050503678
License date	Aug 23, 2019
Licensed Content Publisher	Elsevier
Licensed Content Publication	Elsevier Books

Licensed Content Title	Cartilage Surgery
Licensed Content Author	Mats Brittberg
Licensed Content Date	Jan 1, 2011

Figure 2.6-Table listing the advantages and disadvantages of the main OA and damaged cartilage treatment options

Obtained from the Open access article, "Articular cartilage: Structure, Composition, Injuries and repair", by Hooi Yee Ng, Kai-Xing Alvin Lee and Yu-Fang Shen [26] in SciMedCentral-JSM Bone and Joint Diseases.

Figure 2.7-Chemical structure of Inorganic polyphosphate

Journal of cell science

- **Order detail ID:**71995015
- **ISSN:**1477-9137
- **Publication Type:** e-Journal
- **Publisher:** COMPANY OF BIOLOGISTS LTD.
- **Author/Editor:** Company of Biologists
- **Permission Status:** **Granted**
- **Permission type:** Republish or display content

- **Type of use:** Republish in a thesis/dissertation

Order License Id: 4657460401383